

**SOME EFFECTIVE OPERATORS
FOR GRAPHENE MONOLAYER SUPERLATTICES,
FROM VARIATIONAL PERTURBATION THEORY**

LOUIS GARRIGUE

ABSTRACT. Our goal is to provide precise effective operators for monolayer graphene at Fermi energy. We consider the microscopic potential created by a lattice, and add a macroscopic potential with the same periodicity but varying at a scale $\varepsilon^{-1} \in \mathbb{N}$, creating a superlattice. Our approach consists in coupling the variational approximation, perturbation theory together with a multiscale method. At the effective level the usual massless Dirac operator is replaced by other operators, and we provide simulations in the case of graphene.

1. INTRODUCTION

In this document, we consider semiclassical Schrödinger operators of the form

$$h^\varepsilon := \frac{1}{2}(-i\nabla + \varepsilon A(\varepsilon x))^2 + v(x) + \varepsilon V(\varepsilon x), \quad (1)$$

where v , V and A are Ω -periodic potentials having the same periodicity. When ε becomes small, the spectrum of (1) is numerically hard to reach because the periodicity cell is $\varepsilon^{-1}\Omega$, hence one needs to develop effective models. We will be interested in the states at the interface between filled and unfilled bands, because they are the main ones determining the physical behavior of quantum systems. In particular, this applies to graphene considered as a one-body model like in DFT.

The physics literature investigated those doubly periodic systems, called monolayer superlattices, enabling a better control on the propagation of electronic waves for graphene, with periodic electric potentials [5, 18, 27, 37, 38, 58, 80, 81], magnetic ones [11, 12, 14, 28, 29, 57, 76, 84, 86] for instance to compute the mini-band structures [4, 18, 49, 59, 70, 71, 85], or transport properties [16, 19, 25]. We will often take $A = 0$ for simplicity. It is well-known that the effective operator modeling particles around the Fermi level, for only one valley, is then a massless Dirac operator in the potential V , i.e. it is

$$v_F \sigma \cdot (-i\nabla) + V,$$

where $\sigma := (\sigma_1, \sigma_2)$ are the Pauli matrices, and $v_F \in \mathbb{R}_+$ is the graphene Fermi velocity, see for instance [49, (2)]. Notice that in some articles, authors start from $\frac{1}{2}(-\Delta) + v(x) + V(\varepsilon x)$ and derive $v_F \sigma \cdot (-i\nabla) + \frac{1}{\varepsilon}V(x)$ but this involves a singular potential $\frac{1}{\varepsilon}V$ so here we rather start from (1) and at the end one can formally replace $V \rightarrow \frac{1}{\varepsilon}V$. This approach of modulating monolayer graphene

using a parametrized larger scale potential provides an alternative to moiré systems to obtain precise control over the electronic behavior. Moreover, a macroscopic periodic modulation of monolayer graphene is a first step before a better understanding of bilayer moirés [23], relaxed graphene (see [56, p58], [64, eq. (45)], [51, Chapter 9, p213]) or two untwisted microscopic lattices with different lattice constants [52, 68].

The mathematics literature also contains works on the study of (1), or in the scaling $\frac{1}{2}(-i\nabla + A(\varepsilon x))^2 + v(x) + V(\varepsilon x)$. The derivation of effective models for graphene at the macroscopic scale was done using semiclassical techniques in [20, 30, 41, 43], a dynamical approach in [3, 36, 42, 69], and in a spectral approach in [34] in the strong binding regime. The case of twisted bilayer graphene received a lot of attention, derivations of effective operators for twisted bilayer graphene began with the Bistritzer-MacDonald model [15], which was mathematically studied in [6–9]. Other derivations were done in [21, 22, 54, 74, 82], and in [75] for higher-order models. To develop effective models in multiscale situations, reduced basis methods were applied in homogenization [17, 26, 46, 65, 67], and ideas from multiscale finite element method [1, 32, 48] were applied to semiclassical Schrödinger operators [24, 60].

In [21], the authors used a variational approximation which produced an effective operator $v_F \sigma \cdot (-i\nabla) + \frac{1}{2}\varepsilon(-\Delta) + V$. The variational space consisted in functions of the form $\sum_{a=1}^2 \alpha_a(x) \phi_a\left(\frac{x}{\varepsilon}\right)$, where α is left free and ϕ_1 and ϕ_2 are the Bloch eigenfunctions at the Dirac point corresponding to the Fermi energy. The variational space is hence free at the macroscopic level but imposed at the microscopic level. In this document, we use the same approach but also couple it to perturbation theory. To the best of our knowledge, the coupling between the variational approximation and perturbation theory was first used in [66]. It is now used in the physics literature [31, 39], and a mathematical analysis of this method is provided in [40]. To develop an improved variational space for (1), we enrich the microscale functions by not only inserting the Bloch eigenfunctions at the Dirac point, but also their derivatives with respect to the momentum parameter k . We hence do not obtain a 2×2 -valued matrix operator but an $M \times M$ -valued one, where M is the number of functions in the microscale basis. For instance, corresponding to order one in perturbation theory, one can add 4 derivatives (two perturbation directions for two states), resulting in a 6×6 -matrix valued effective operator presented in Section 4.5.

We introduce the problem in Section 2, then in Section 3 we present the general effective operators. In Section 4 we take particular cases for deriving effective operators. Finally in Section 5 we display some simulations for the band diagrams, showing that the effective operators derived in this document provide more accurate band diagrams and eigenvectors than the traditional massless Dirac operator.

2. INTRODUCTION OF THE SETTING

In this section we introduce the objects that will be manipulated, most importantly we present the scaled exact operator.

2.1. The lattice. We consider the two-dimensional space \mathbb{R}^2 instead of \mathbb{R}^3 in which graphene is embedded, but everything can be extended to the \mathbb{R}^3 situation. Let us consider $a_0 > 0$, $k_D := \frac{4\pi}{3a_0}$, and the graphene lattice vectors

$$a_1 := a_0 \begin{pmatrix} \frac{1}{2} \\ -\frac{\sqrt{3}}{2} \end{pmatrix}, \quad a_2 := -a_0 \begin{pmatrix} \frac{1}{2} \\ \frac{\sqrt{3}}{2} \end{pmatrix}, \quad (2)$$

$$a_1^* := \sqrt{3}k_D \begin{pmatrix} \frac{\sqrt{3}}{2} \\ -\frac{1}{2} \end{pmatrix}, \quad a_2^* := -\sqrt{3}k_D \begin{pmatrix} \frac{\sqrt{3}}{2} \\ \frac{1}{2} \end{pmatrix}. \quad (3)$$

We define the action of \mathbb{R}^2 on a_1 and a_2 as $na := n_1a_1 + n_2a_2$ and similarly $ma^* := m_1a_1^* + m_2a_2^*$. The direct lattice is $\mathbb{L} := \{na \mid n \in \mathbb{Z}^2\}$, the dual one is thus $\mathbb{L}^* := \{ma^* \mid m \in \mathbb{Z}^2\}$. The fundamental cell is $\Omega := \{xa \mid x \in [0, 1]^2\}$ and we denote by \mathcal{B} the first Brillouin zone. We will consider the Dirac point $K := -\frac{1}{3}(a_1^* + a_2^*) \in \mathcal{B}$, a high-symmetry point.

2.2. Scaling. For any $n \in \mathbb{N}$ and any $q \in [1, +\infty[$, we define the set of periodic operators

$$L_{\text{per}}^q(n\Omega) := \{f \in L_{\text{loc}}^q(\mathbb{R}^2) \mid \forall x \in \mathbb{R}^2, \forall y \in \mathbb{L}, f(x + ny) = f(x)\}.$$

For any $n \in \mathbb{N}$ and any function $f, g \in L_{\text{per}}^2(\varepsilon^{-1}\Omega)$, we define $\langle f, g \rangle_{L_{\text{per}}^2(n\Omega)} := \int_{n\Omega} \bar{f}g$. Moreover, we will use mainly

$$\langle \cdot, \cdot \rangle := \langle \cdot, \cdot \rangle_{L_{\text{per}}^2(\Omega)}.$$

We define the scaling operator Q on functions $f : \mathbb{R}^2 \rightarrow \mathbb{R}$ by

$$(Qf)(x) := f\left(\frac{x}{\varepsilon}\right),$$

its inverse is $(Q^{-1}f)(x) = f(\varepsilon x)$. We have $Q : L_{\text{per}}^2(\varepsilon^{-1}\Omega) \rightarrow L_{\text{per}}^2(\Omega)$ and for $\varepsilon \in 1/\mathbb{N} := \{1/n, n \in \mathbb{N} \setminus \{0\}\}$, $\langle Qf, Qg \rangle_{L_{\text{per}}^2(\Omega)} = \varepsilon^2 \langle f, g \rangle_{L_{\text{per}}^2(\varepsilon^{-1}\Omega)}$ so in those spaces, $Q^* = \varepsilon^2 Q^{-1}$.

2.3. Symmetries of the potentials. Let us define the rotation matrix

$$R_\theta := \begin{pmatrix} \cos \theta & -\sin \theta \\ \sin \theta & \cos \theta \end{pmatrix},$$

and its corresponding action $(\mathcal{R}_\theta f)(x) := f(R_{-\theta}x)$ on functions $f : \mathbb{R}^2 \rightarrow \mathbb{R}$. We consider potentials with honeycomb symmetry, which is defined in [35, Definition 2.1]. They are potentials $v \in L^p(\mathbb{R}^2)$, with $p > 1$, such that

$$v \in L_{\text{per}}^p(\Omega), \quad v(-x) = v(x), \quad \mathcal{R}_{\frac{2\pi}{3}}v = v, \quad v(x_1, -x_2) = v(x_1, x_2). \quad (4)$$

As for the potentials V and A , we only assume that $V, A \in L_{\text{per}}^p(\Omega)$ but for simulations of Section 5 we will choose $A = 0$ and V respecting the symmetries (4).

2.4. The scaled exact operator.

2.4.1. *The microscopic exact problem.* Let us denote by $(E_m^q, u_m^q) \in \mathbb{R} \times H_{\text{per}}^1(\Omega)$ the Bloch eigenpairs of

$$h_q := \frac{1}{2}(-i\nabla_q)^2 + v, \quad \mathbb{L} - \text{periodic},$$

which is bounded from below, for $m \in \mathbb{N}$ and $q \in \mathcal{B}$, sorted such that E_m^q is increasing with m . Hence

$$h_q u_m^q = E_m^q u_m^q. \quad (5)$$

We assume that there is $m_F \in \mathbb{N}$ such that the dispersion relation of $k \mapsto h_k$ has a conical intersection at the Dirac point $k = K$ at the level m_F . This situation is generic, as proved in [35, Theorem 5.1]. In particular, this implies that $E_{m_F}^K = E_{m_F+1}^K =: E_F$, which we call the Fermi level. We also assume that this level is exactly 2-fold degenerate, so $E_{m_F-1}^K < E_{m_F}^K = E_{m_F+1}^K < E_{m_F+2}^K$.

Let us define

$$w_1 := u_{m_F}^K, \quad w_2 := u_{m_F+1}^K \quad (6)$$

such that $\|w_1\|_{L_{\text{per}}^2(\Omega)} = \|w_2\|_{L_{\text{per}}^2(\Omega)} = 1$ and such that with

$$\phi_a(x) := e^{iKx} w_a(x), \quad (7)$$

we have

$$\mathcal{R}_{\frac{2\pi}{3}} \phi_a = \omega^a \phi_a, \quad \text{for all } a \in \{1, 2\}, \quad (8)$$

where $\omega := e^{i\frac{2\pi}{3}}$, see [35]. The functions ϕ_1 and ϕ_2 are the Bloch states at the Dirac point and Fermi level, see [35] for more details about the symmetries of those Bloch states.

2.4.2. *The exact operator.* We want to study the operator $h^\varepsilon = -\frac{1}{2}\Delta + v + \varepsilon Q^{-1}V$ defined in (1), which is $\varepsilon^{-1}\mathbb{L}$ -periodic. For any $q \in \mathbb{R}^2$, we define $\nabla_q := e^{-iqx}\nabla e^{iqx}$ where e^{iqx} is considered as a multiplication operator, so $\nabla_q = \nabla + iq$ and $-i\nabla_q = -i\nabla + q$. Instead of h^ε , we work on its Bloch transform, acting on $L_{\text{per}}^2(\varepsilon^{-1}\Omega)$ and given by

$$h_q^\varepsilon = e^{-iqx} h^\varepsilon e^{iqx} = \frac{1}{2}(-i\nabla_q + \varepsilon Q^{-1}A)^2 + v + \varepsilon Q^{-1}V. \quad (9)$$

We have $\nabla_q Q = \varepsilon^{-1}Q\nabla_{\varepsilon q}$ so $\varepsilon Q^{-1}\nabla_{\varepsilon^{-1}q} = \nabla_q Q^{-1}$, $(-i\nabla_q + Q^{-1}A)^2 Q^{-1} = \varepsilon^2 Q^{-1}(-i\nabla_{\varepsilon^{-1}q} + A)^2$ and instead of h_q^ε we work on its rescaled (and hence semiclassical) version $Qh_q^\varepsilon Q^{-1}$. We center the study of h^ε around the Fermi level, which we assume to be at a the Dirac point K , presenting a conical intersection in the dispersion relation, see [35] for a precise definition. Hence we work on

$$H_k^\varepsilon := Q(h_{K+\varepsilon k}^\varepsilon - E_F)Q^{-1} = \frac{1}{2}\varepsilon^2(-i\nabla_{\varepsilon^{-1}K+k} + A)^2 + Qv + \varepsilon V - E_F, \quad (10)$$

which acts on $L_{\text{per}}^2(\Omega)$. The two operations ‘‘scaling’’ and ‘‘Bloch transform’’ commute, hence the order in which we apply them does not matter.

2.4.3. *Exact eigenvectors when $V = 0$.* Let us denote by $H_k^{\varepsilon, V=0}$ the operator H_k^ε with $V = 0$. In this case, its band diagram is simply a folding of the band diagram of $-\frac{1}{2}\Delta + v$, (see [33, 55, 62, 73] for the folding/unfolding operations) and the eigenmodes of $H_k^{\varepsilon, V=0}$ can be deduced from the ones of $-\frac{1}{2}(-i\nabla_p) + v$. Let us analyze the branches starting at the Dirac point. We compute that $H_k^{\varepsilon, V=0} Q u_m^{K+\varepsilon k} = (E_m^{K+\varepsilon k} - E_F) Q u_m^{K+\varepsilon k}$, so $(E_m^{K+\varepsilon k} - E_F, Q u_m^{K+\varepsilon k})_{m \in \mathbb{N}}$ are eigenmodes for $H_k^{\varepsilon, V=0}$. Moreover if V is considered as a perturbation, the eigenmodes of $H_k^{\varepsilon, V=0}$ are smoothly deformed to the ones of H_k^ε .

3. THE GENERAL EFFECTIVE OPERATORS

In this section we present effective operators for two-scales graphene, in a general way. More specific choices will be made in Section 4.

3.1. **Two-scales reduced basis.** Let us consider a family \mathcal{F} of M linearly independent and periodic functions $\psi_1, \dots, \psi_M \in H_{\text{per}}^1(\Omega)$,

$$\mathcal{F} := (\psi_j)_{1 \leq j \leq M}. \quad (11)$$

This family will impose the behaviors of eigenfunctions of the reduced space at the microscopic scale. They potentially depend on the momentum k , but not on ε . As in [21], we then build the reduced vector space

$$\left\{ \sum_{j=1}^M \alpha_j(x) \psi_j\left(\frac{x}{\varepsilon}\right) \mid \alpha_j \in \mathcal{C}_{\text{per}}^\infty(\Omega), j \in \{1, \dots, M\} \right\}, \quad (12)$$

which is the two-scale space “spanned” by the space of microscopic functions of \mathcal{F} when the macroscopic behavior is left free. Efficient families will

- have M small so the resulting effective model will be “computable”,
- choose ψ_j in a way so that the resulting effective operator will be accurate.

We then define the operator

$$\mathcal{J} : \begin{array}{ccc} \mathbb{C}^M \otimes \mathcal{C}_{\text{per}}^\infty(\Omega, \mathbb{C}) & \longrightarrow & H_{\text{per}}^1(\Omega, \mathbb{C}) \\ \alpha & \longmapsto & \sum_{j=1}^M \alpha_j(x) \psi_j\left(\frac{x}{\varepsilon}\right), \end{array}$$

which enables to go from envelop functions to real-space functions.

3.2. **Effective operator.** We study the action of the exact operator H_k^ε in the projected space (12). We want to associate it a low-dimensional model which will reproduce the Fermi eigenmodes with precision. Let us define

$$\begin{aligned} \mathcal{M} &:= (\langle \psi_a, (h_k - E_F) \psi_b \rangle)_{1 \leq a, b \leq M}, & \mathcal{S} &:= (\langle \psi_a, \psi_b \rangle)_{1 \leq a, b \leq M} \\ \mathcal{L} &:= (\langle \psi_a, (-i\nabla_K) \psi_b \rangle)_{1 \leq a, b \leq M}, \end{aligned}$$

where the coefficients of \mathcal{L} belong to \mathbb{C}^2 . Those $M \times M$ matrices are all hermitian, \mathcal{S} is a Gram matrix, so since \mathcal{F} is composed of linearly independent functions, \mathcal{S} is strictly positive. Then an effective model for H_k^ε is

$$\mathbb{H}_k^\varepsilon := \varepsilon^{-1} \mathcal{M} \otimes \mathbb{1} + \mathcal{L} \cdot \otimes (-i\nabla_k + A) + \mathcal{S} \otimes \left(\frac{1}{2} \varepsilon (-i\nabla_k + A)^2 + V \right) \quad (13)$$

as an operator of $\mathbb{C}^M \otimes \mathcal{C}_{\text{per}}^\infty(\Omega)$, where the only spatial dependence exists via V and A . A formal derivation of (13) is provided by the following proposition.

Proposition 3.1 (Weak convergence). *Take $\alpha, \beta \in \mathbb{C}^M \otimes \mathcal{C}_{\text{per}}^\infty(\Omega)$, and $V, A \in \mathcal{C}_{\text{per}}^\infty(\Omega)$. For any $N \in \mathbb{N}$, there exists $C_N > 0$ such that for any $\varepsilon \in]0, 1[\cap(1/\mathbb{N})$,*

$$\left| \varepsilon^{-1} |\Omega| \langle \mathcal{J}\alpha, H_k^\varepsilon \mathcal{J}\beta \rangle_{L^2_{\text{per}}(\Omega, \mathbb{C})} - \langle \alpha, \mathbb{H}_k^\varepsilon \beta \rangle_{\mathbb{C}^M \otimes L^2_{\text{per}}(\Omega, \mathbb{C})} \right| \leq C_N \varepsilon^N.$$

A proof is given in Section 6. The eigenvalue equation for \mathbb{H}_k^ε is then

$$\mathbb{H}_k^\varepsilon \alpha_k^\varepsilon = \mathbb{E}_k^\varepsilon \mathcal{S} \alpha_k^\varepsilon,$$

where the generalized eigenpairs of \mathbb{H}_k^ε will be denoted by $(\mathbb{E}_k^\varepsilon, \alpha_k^\varepsilon)$. When \mathcal{F} is well chosen, the operator \mathbb{H}_k^ε spectrally well approximates the exact operator H_k^ε in the following sense : if V and A are small enough and if $(\mathbb{E}_k^\varepsilon, \alpha_k^\varepsilon)$ is a generalized eigenpair of \mathbb{H}_k^ε , then there exists an eigenpair $(\mathcal{E}_k^\varepsilon, \Phi_k^\varepsilon)$ of H_k^ε such that

$$\varepsilon^{-1} (\mathcal{E}_k^\varepsilon - \mathcal{E}_0^\varepsilon) \simeq \mathbb{E}_k^\varepsilon - \mathbb{E}_0^\varepsilon, \quad \Phi_k^\varepsilon \simeq \mathcal{J} \alpha_k^\varepsilon \text{ up to a phase factor.}$$

The maps $(k, V) \mapsto \mathcal{E}_k^\varepsilon$ and $(k, V) \mapsto \mathbb{E}_k^\varepsilon$ are locally smooth away from eigenvalue crossings. So to detect which level of the effective model corresponds to which one of the exact model, we start by identifying the eigenmodes of $H_0^{\varepsilon, V=0}$ and $\mathbb{H}_0^{\varepsilon, V=0}$ (see Section 2.4.3), which eigenvalues then vanish, and then we let k and V change smoothly to see the deformations of eigenvalues and keep track of them even at crossings.

Remark 3.2 (Undo the Bloch transform). *When the coefficient matrices \mathcal{M}, \mathcal{L} and \mathcal{S} do not depend on k , the operator in real space can be written as the inverse of the Bloch transform $\mathbb{H}^\varepsilon = e^{ikx} \mathbb{H}_k^\varepsilon e^{-ikx}$ and does not depend on k .*

Remark 3.3 (Effective operators are defined for any $\varepsilon > 0$). *While the exact operator H_k^ε is only defined for $\varepsilon \in 1/\mathbb{N}$, the effective operators \mathbb{H}_k^ε are defined for any $\varepsilon > 0$. Moreover, the computation cost of the effective operators is essentially constant in ε while it was exponentially increasing with $1/\varepsilon$ in the exact model.*

3.3. First simplification. We recall the Pauli matrices

$$\sigma_1 := \begin{pmatrix} 0 & 1 \\ 1 & 0 \end{pmatrix}, \quad \sigma_2 := \begin{pmatrix} 0 & -i \\ i & 0 \end{pmatrix}, \quad \sigma_3 := \begin{pmatrix} 1 & 0 \\ 0 & -1 \end{pmatrix}.$$

In our choices of \mathcal{F} , for any k we will always have $\psi_a = w_a$ for $a \in \{1, 2\}$, where w_a are the Bloch states at the point K , defined in Section 2.4.1. We will also always have $w_a \perp \psi_b$ for $a \in \{1, 2\}$ and $b \in \{3, \dots, M\}$. Hence the operators \mathcal{M}, \mathcal{L} and \mathcal{S} can be simplified as

$$\mathcal{M} = \begin{pmatrix} 0 & 0 \\ 0 & M \end{pmatrix}, \quad \mathcal{L} = \begin{pmatrix} v_F \sigma & T \\ T^* & L \end{pmatrix}, \quad \mathcal{S} = \begin{pmatrix} \mathbb{1} & 0 \\ 0 & S \end{pmatrix}. \quad (14)$$

where

$$\begin{aligned} S &:= (\langle \psi_{a+2}, \psi_{b+2} \rangle)_{1 \leq a, b \leq M-2}, & M &:= (\langle \psi_{a+2}, (h_k - E_F) \psi_{b+2} \rangle)_{1 \leq a, b \leq M-2} \\ T &:= (\langle \psi_a, (-i \nabla_K) \psi_{b+2} \rangle)_{\substack{1 \leq a \leq 2 \\ 1 \leq b \leq M-2}}, & L &:= (\langle \psi_{a+2}, (-i \nabla_K) \psi_{b+2} \rangle)_{1 \leq a, b \leq M-2}. \end{aligned} \quad (15)$$

Moreover, $v_F \in \mathbb{R}_+$ is defined via $\langle w_1, (-i \nabla_K) w_2 \rangle = v_F (1, -i)^T$, see [21, Appendix I].

4. PARTICULAR EFFECTIVE MODELS

From now on we take $A = 0$.

4.1. Preliminary information about the unscaled system. In this section, we present particular choices for the families \mathcal{F} defined in (11), which will implement a multiscale variational perturbation theory.

4.1.1. *A family of Bloch eigenmodes with special symmetry.* From [10, 35], the symmetries of w_a presented in Section 2.4.1 imply that

$$\langle w_a, (-i\nabla_K)w_a \rangle = 0, \quad a \in \{1, 2\}, \quad \langle w_1, (-i\nabla_K)w_2 \rangle = v_F \begin{pmatrix} 1 \\ -i \end{pmatrix}. \quad (16)$$

Those computations are enough to derive the effective massless Dirac operator $v_F \sigma \cdot (-i\nabla)$ from $-\frac{1}{2}\Delta + v$ where v has honeycomb symmetry.

4.1.2. *Pseudo-inverse.* Let us denote by P the orthogonal projector onto the eigenspace $\text{Ker}(h_K - E_F) = \text{Span}(w_1, w_2)$, and $P_\perp := 1 - P$. An important quantity which we will need is the pseudo-inverse

$$R := \begin{cases} \left((E_F - h_K)|_{P_\perp L_{\text{per}}^2(\Omega) \rightarrow P_\perp L_{\text{per}}^2(\Omega)} \right)^{-1} & \text{on } P_\perp L_{\text{per}}^2(\Omega) \\ 0 & \text{on } PL_{\text{per}}^2(\Omega) \end{cases}$$

extended on $L_{\text{per}}^2(\Omega)$ by linearity, so $(E_F - h_K)R = R(E_F - h_K) = P_\perp$.

4.2. Variational perturbation theory : Dirac modes and their derivatives up to order ℓ . The first way of building families \mathcal{F} comes from variational perturbation theory [39, 66], which was analyzed mathematically in [40]. It consists in building a variational space using the derivatives of the eigenfunctions. Here we build \mathcal{F} using $u_{m_F}^q$ and their derivatives with respect to q . In Appendix B we present how one can differentiate those eigenstates with respect to q at $q = K$.

For any $k \in \mathbb{R}^2 \setminus \{0\}$, we will use the differentiation operator in direction $\frac{k}{|k|}$ denoted by

$$D_k := \frac{k}{|k|} \cdot (-i\nabla_K),$$

where we recall that $\nabla_K = \nabla + iK$. We use the notation $\partial_{K,j} = (\nabla_K)_j = \partial_j + iK_j$. Labeling the first index of \mathcal{F} by the perturbative order, we define, for any direction $k \in \mathbb{R}^2 \setminus \{0\}$,

$$\begin{aligned} \mathcal{F}_0 &:= (w_1, w_2), & \mathcal{F}_{1,k} &:= (w_1, w_2, RD_k w_1, RD_k w_2), & (17) \\ \mathcal{F}_1 &:= (w_1, w_2, R(-i\partial_{K,1})w_1, R(-i\partial_{K,2})w_1, R(-i\partial_{K,1})w_2, R(-i\partial_{K,2})w_2), \\ \mathcal{F}_{2,k} &:= \{w_a, RD_k w_a, (RD_k)^2 w_a - R^2 D_k P D_k w_a\}_{1 \leq a \leq 2} \\ \mathcal{F}_2 &:= \{w_a, R(-i\partial_{K,b})w_a, R^2(-i\partial_{K,b})w_a, R(-i\partial_{K,b})R(-i\partial_{K,c})w_a\}_{1 \leq a, b, c \leq 2}. \end{aligned}$$

Remark that the vectors of the families $\mathcal{F}_{\ell,k}$ depend on k only via the direction $\frac{k}{|k|}$. We have $|\mathcal{F}_0| = 2$, $|\mathcal{F}_{1,k}| = 4$, $|\mathcal{F}_1| = |\mathcal{F}_{2,k}| = 6$, $|\mathcal{F}_2| = 18$. As explained in Appendix B, each \mathcal{F}_ℓ and $\mathcal{F}_{\ell,k}$ contain the directional derivatives of $q \mapsto u_{m_F}^q$

up to order ℓ at $q = K$, and Section 8 gives a justification of this choice. More precisely, those spaces are built such that for $\ell \in \{0, 1, 2\}$,

$$u_{m_F}^{K+k} = U + O_{|k| \rightarrow 0}(|k|^{\ell+1}), \quad \text{where } U \in \text{Span } \mathcal{F}_{\ell,k} \subset \text{Span } \mathcal{F}_\ell.$$

Following the method presented in Section B.3, one can similarly build families $\mathcal{F}_{\ell,k}$ at all perturbative orders ℓ .

4.3. Order 0. The family \mathcal{F}_0 is the choice made in [21, Remark 1]. Then the effective model consists in a massless Dirac operator

$$\mathbb{H}_k^\varepsilon = v_F \sigma \cdot (-i\nabla_k) + V + \frac{1}{2}\varepsilon(-i\nabla_k)^2.$$

4.4. Order 1, k -dependent. We want to compute the matrices S , M , L and T defined in (15) and which are sufficient to describe the effective operator.

For any $q = (q_1, q_2) \in \mathbb{R}^2$, we define $q_{\mathbb{C}} := q_1 + iq_2$. For any $k \in \mathcal{B} \setminus \{0\}$, let us define $\theta_k \in [0, 2\pi[$ such that $k_{\mathbb{C}} = |k|e^{i\theta_k}$. Let us define

$$\begin{aligned} t &:= \|R(-i\partial_{K,1})w_1\|^2, & t' &:= \langle (-i\partial_{K,1})w_1, R(-i\partial_{K,1})w_1 \rangle, \\ r &:= \langle R(-i\partial_{K,1})w_1, R(-i\partial_{K,1})w_2 \rangle, & r' &:= \langle (-i\partial_{K,1})w_1, R(-i\partial_{K,1})w_2 \rangle, \\ s &:= \langle R(-i\partial_{K,2})w_1, R(-i\partial_{K,1})w_1 \rangle, & s' &:= \langle (-i\partial_{K,2})w_1, R(-i\partial_{K,1})w_1 \rangle, \end{aligned} \quad (18)$$

and

$$\begin{aligned} \chi &:= \langle R(-i\partial_{K,1})w_1, (-i\partial_{K,1})R(-i\partial_{K,1})w_1 \rangle, \\ \gamma_1 &:= \langle R(-i\partial_{K,1})w_1, (-i\partial_{K,2})R(-i\partial_{K,2})w_2 \rangle, \\ \gamma_2 &:= \langle R(-i\partial_{K,2})w_1, (-i\partial_{K,1})R(-i\partial_{K,2})w_2 \rangle. \end{aligned} \quad (19)$$

Proposition 4.1 (Effective matrices for $\mathcal{F}_{1,k}$). *In the case $\mathcal{F}_{1,k}$, we have that $r, t', r', s, s', \chi, \gamma_1, \gamma_2 \in \mathbb{R}$ and the matrices defined in (15) are*

$$S = \begin{pmatrix} t & r e^{i2\theta_k} \\ r e^{-i2\theta_k} & t \end{pmatrix}, \quad M = - \begin{pmatrix} t' & r' e^{i2\theta_k} \\ r' e^{-i2\theta_k} & t' \end{pmatrix} \quad (20)$$

$$T = \begin{pmatrix} (t'\mathbf{1} - s'\sigma_2) \frac{k}{|k|} & r' e^{i\theta_k} \begin{pmatrix} 1 \\ i \end{pmatrix} \\ r' e^{-i\theta_k} \begin{pmatrix} 1 \\ -i \end{pmatrix} & (t'\mathbf{1} + s'\sigma_2) \frac{k}{|k|} \end{pmatrix}, \quad (21)$$

and using $\sigma = (\sigma_1, \sigma_2)$,

$$L = \begin{pmatrix} \chi \begin{pmatrix} \cos(2\theta_k) \\ -\sin(2\theta_k) \end{pmatrix} & 2\gamma_1 e^{-i\theta_k} \begin{pmatrix} \cos \theta_k \\ \sin \theta_k \end{pmatrix} \\ 2\gamma_1 e^{i\theta_k} \begin{pmatrix} \cos \theta_k \\ \sin \theta_k \end{pmatrix} & \chi \begin{pmatrix} \cos(2\theta_k) \\ -\sin(2\theta_k) \end{pmatrix} \end{pmatrix} + \gamma_2 \sigma. \quad (22)$$

The computations are provided in Section 7.4. A drawback is that the effective matrices are not defined for $k = 0$.

4.5. Order 1, k -independent. We choose \mathcal{F}_1 , its vectors in the order presented in (17), that is $\psi_1 = w_1$, $\psi_2 = w_2$, $\psi_3 = R(-i\partial_{K,1})w_1$, $\psi_4 = R(-i\partial_{K,2})w_1$, $\psi_5 = R(-i\partial_{K,1})w_2$, $\psi_6 = R(-i\partial_{K,2})w_2$.

Proposition 4.2 (Effective matrices for \mathcal{F}_1). *In the case \mathcal{F}_1 , with the same constants as in (18) and (19), which are still real, the matrices defined in (15) are*

$$S = \begin{pmatrix} t\mathbb{1} + s\sigma_2 & rD \\ rD^* & t\mathbb{1} - s\sigma_2 \end{pmatrix}, \quad M = - \begin{pmatrix} t'\mathbb{1} + s'\sigma_2 & r'D \\ r'D^* & t'\mathbb{1} - s'\sigma_2 \end{pmatrix}$$

and $T = (T^1, T^2)$ and $L = (L^1, L^2)$ with

$$T^1 = \begin{pmatrix} t' & -is' & r' & ir' \\ r' & ir' & t' & is' \end{pmatrix}, \quad T^2 = \begin{pmatrix} is' & t' & ir' & -r' \\ ir' & -r' & -is' & t' \end{pmatrix}$$

and

$$L^1 = \begin{pmatrix} \chi & 0 & 2\gamma_1 + \gamma_2 & -i\gamma_1 \\ 0 & -\chi & -i\gamma_1 & \gamma_2 \\ 2\gamma_1 + \gamma_2 & i\gamma_1 & \chi & 0 \\ i\gamma_1 & \gamma_2 & 0 & -\chi \end{pmatrix}, \quad L^2 = \begin{pmatrix} 0 & -\chi & -i\gamma_2 & \gamma_1 \\ -\chi & 0 & \gamma_1 & -i(2\gamma_1 + \gamma_2) \\ i\gamma_2 & \gamma_1 & 0 & -\chi \\ \gamma_1 & i(2\gamma_1 + \gamma_2) & -\chi & 0 \end{pmatrix}.$$

The proof is similar to the one of Proposition 4.1 and uses Lemmas 7.3 and 7.4.

4.6. Values of the parameters for graphene. We computed the values of those effective parameters with the software DFTK [45], which uses DFT to obtain the vectors u_m^K , we took the case of physical standard graphene. This provides the following values, which are expressed in electronvolt

$$\begin{aligned} r &= -30 \text{ eV}, & t &= 32 \text{ eV}, & s &= 29 \text{ eV}, \\ r' &= 13 \text{ eV}, & t' &= -15 \text{ eV}, & s' &= -11 \text{ eV}, \\ \chi &\simeq -2 \cdot 10^{-2} \text{ eV}, & \gamma_1 &= -1.2 \text{ eV}, & \gamma_2 &= 0.6 \text{ eV} \end{aligned}$$

This numerical value of χ is not very precise. With our tool, we also obtain $v_F = 11 \text{ eV}$.

4.7. Using excited states. We can also form families \mathcal{F} of microscopic functions from Bloch eigenstates at the Dirac point. For $p \in \mathbb{N}$, $p \geq 3$, we will study

$$\mathcal{F}^n := (u_a^K)_{a \in \{m_F, \dots, m_F + n - 1\}}. \quad (23)$$

We have $|\mathcal{F}^n| = n$ and remark that $\mathcal{F}^2 = \mathcal{F}_0$. We recall that the usual Bloch eigenfunctions studied in [35] are $w_a = u_{m_F + a - 1}^K$ for $a \in \{1, 2\}$. We define $w_3 := u_{m_F + 2}^K$ and we only explicitly write the case $\mathcal{F}^3 = \{w_1, w_2, w_3\}$. In general, the energy $E^3 := E_{m_F + 2}^K = \langle w_3, h_K w_3 \rangle$ is different to the Fermi energy E_F , and $\phi_3(x) := e^{iKx} w_3(x)$ can be defined as in (7) and let us assume that ϕ_3 is in a different representation of $\mathcal{R}_{\frac{2\pi}{3}}$ than ϕ_1 and ϕ_2 so assume that $\mathcal{R}_{\frac{2\pi}{3}} \phi_3 = \phi_3$. The only additional parameter is $\tilde{v}_F := -i \langle w_1, (-i\partial_{K,1})w_3 \rangle$.

We define the parity and complex conjugation operators $(\mathcal{P}f)(x) := f(-x)$, $(\mathcal{C}f)(x) := \bar{f}(x)$.

Proposition 4.3 (Effective matrices for \mathcal{F}^3). *In the case \mathcal{F}^3 and assuming that $\mathcal{CP}\phi_3 = \phi_3$, the matrices defined in (15) are $S = 1$, $M = E^3 - E_{\mathbb{F}}$, $L = 0$ and*

$$T = -\tilde{v}_{\mathbb{F}} \begin{pmatrix} (-i) \\ \frac{1}{i} \\ \frac{1}{i} \end{pmatrix},$$

where $\tilde{v}_{\mathbb{F}} \in \mathbb{R}$.

The computations are provided in Section 7.5. We see that one advantage of this kind of choice is that the effective matrices are simple and involve few constants to compute.

4.8. Exact modes at each k . Another natural choice is to take the family $\mathcal{F} = \{u_{m_{\mathbb{F}}}^k, u_{m_{\mathbb{F}}+1}^k\}$, it has the benefit to be an exact choice when $V = 0$, so the eigenmodes of the effective operators give some of the exact ones. But the drawback is that in this case one needs to solve h_k at each k in the Brillouin zone. We will not explore this choice in the numerical investigation.

4.9. Error and limit of high M . Let us denote by $P_{\mathcal{J}}$ the orthogonal projection onto $\text{Im } \mathcal{J}$, and $P_{\mathcal{J}}^{\perp} := 1 - P_{\mathcal{J}}$. We recall that we denoted by Φ_k^{ε} the eigenvector of the exact operator H_k^{ε} defined in (10). As presented in [2, Chapter II, Section 8, (8.46)] or in [40, Proposition 3.2], the error between Φ_k^{ε} and the approximation $\mathcal{J}\alpha_k^{\varepsilon}$ (produced by our effective operators) is controlled by $P_{\mathcal{J}}^{\perp}\Phi_k^{\varepsilon}$. Hence, usually, the larger $\text{Im } \mathcal{J}$ the smaller $P_{\mathcal{J}}^{\perp}\Phi_k^{\varepsilon}$ and the smaller the error $\|\Phi_k^{\varepsilon} - \mathcal{J}\alpha_k^{\varepsilon}\|_{L_{\text{per}}^2(\Omega)}$. So making \mathcal{F} larger improves the approximation but produces effective operators that are more expensive to deal with.

When M is large, one can expect that formally, $\text{Im } \mathcal{J}$ becomes close to

$$\begin{aligned} & \left\{ \sum_{j=1}^M \alpha_j(x) \varphi_j \left(\frac{x}{\varepsilon} \right) \mid \alpha_j \in C_{\text{per}}^{\infty}(\Omega), \varphi_j \in H_{\text{per}}^1(\Omega), j \in \{1, \dots, M\} \right\} \\ & = C_{\text{per}}^{\infty}(\Omega) \otimes H_{\text{per}}^1(\Omega), \end{aligned}$$

and all approximations become equivalent. Hence in the larger M limit, using excited states or derivatives no longer matters.

4.10. Schur reduction to a 2×2 matrix-valued operator. We recall the formalism of Schur's reduction in Appendix C. We formally apply it to the effective operator $\mathbb{H}_k^{\varepsilon}$, where the Schur projection P_2 is the projection onto the first two components of \mathbb{C}^M , the computations are detailed in Section C.1. We define the 2×2 matrix-valued operator

$$\begin{aligned} \mathcal{H}_k^{\varepsilon} & := \mathbf{1} \otimes V + v_{\mathbb{F}} \sigma \otimes \cdot (-i\nabla_k) \\ & \quad + \varepsilon \mathbf{1} \otimes \left(\frac{1}{2} (-i\nabla_k)^2 - T \cdot (-i\nabla_k) (M^{-1} T^*) \cdot (-i\nabla_k) \right), \end{aligned} \quad (24)$$

acting on $\mathbb{C}^2 \otimes L_{\text{per}}^2(\Omega)$, where more precisely, for any $i \in \{1, 2\}$ and any $\psi \in \mathbb{C}^2 \otimes L_{\text{per}}^2(\Omega)$,

$$\begin{aligned} & (T \cdot (-i\nabla_k) (M^{-1} T^*) \cdot (-i\nabla_k) \psi)_i \\ & = \sum_{1 \leq a, b, j \leq 2} \left(T^a M^{-1} (T^b)^* \right)_{ij} (-i\nabla_k)_a (-i\nabla_k)_b \psi_j. \end{aligned}$$

The operator $\mathcal{H}_k^\varepsilon$ is similar to the one derived in [21], but it has a corrected second-order differential operator. It is the operator \mathbb{H}_k^ε on which we applied a Schur reduction, as explained in Appendix C. Hence we “reduced” the operator \mathbb{H}_k^ε , which had divergences, to $\mathcal{H}_k^\varepsilon$, which has no divergence. A drawback of the Schur reductions is that one needs to apply an operator to the eigenvectors of $\mathcal{H}_k^\varepsilon$ to obtain an approximation of the exact eigenvectors, see Appendix C.

5. SIMULATIONS

In this section we are going to explore the way band diagrams vary with change of parameters, and the errors between the effective and exact models. The simulations are done using DFTK [45] but not taking the physical graphene units.

5.1. The parameters. The lattice constant used in (2) will always be $a_0 = 5$. We will use the notation $ma^* := m_1 a_1^* + m_2 a_2^*$. We define $m^1 := (1, 0)$, $m^2 := (0, -1)$, $m^3 := (-1, 1)$ and define the honeycomb potential

$$v_0(x) := 2 \sum_{i=1}^3 \cos((m^i a^*) \cdot x),$$

having the symmetries (4). The microscopic potential will always be the same, $v = 10v_0$. Moreover, the macroscopic one V will mostly be

$$V_{\text{honeycomb}} = \lambda v_0, \quad \lambda \in \mathbb{R}. \quad (25)$$

Our “standard” choice for ε will be $\varepsilon = \frac{1}{7}$. The index of the lower Fermi level will always be $m_F = 1$.

In the band diagrams, the momentum follows a triangular path in momentum space, it will go through $\kappa := (-2, 1)a^*/3$, $\Gamma := (0, 0)$ and $M := -(1, 0)a^*$ as indicated on the horizontal axis, the path will be

$$\kappa \rightarrow \Gamma \rightarrow M \rightarrow \kappa.$$

The vertical axis will represent the energy differences. The origin of energies (i.e. the zero) is chosen such that when $V = 0$, the Fermi level is at zero, for the effective and exact systems.

On Figure 1 we display the band diagram of the exact model when $V = 0$ and $\varepsilon = 1$ (no superlattice).

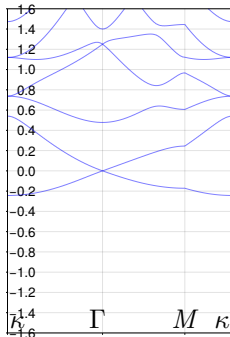


FIGURE 1. Band diagram when $V = 0$ and $\varepsilon = 1$.

5.2. The cutoff ν . We introduce an integer $\nu \in \mathbb{N}$. For $k \in \mathbb{Z}^2$ we define plane waves $p_k(x) := e^{ix \cdot (ka^*)}$ and the set of Ω -periodic functions being composed of momenta lower than ν (in ℓ^∞ norm), more precisely

$$\mathcal{C}_{\text{per},\nu}^\infty := \text{Span}\{p_k \mid k \in \mathbb{Z}^2, \forall i \in \{1, 2\}, |k_i| \leq \nu\}.$$

We actually do not use \mathbb{H}_k^ε defined in (13) but $P_\nu \mathbb{H}_k^\varepsilon P_\nu$ where P_ν is the orthogonal projection onto $\mathbb{C}^M \otimes \mathcal{C}_{\text{per},\nu}^\infty$. This is necessary because increasing M adds undesired bands which pollute the spectrum, as we see on Figure 2. The band of interest is the one coming from the Dirac cone. This first series of band diagrams represents the effective (in black) and exact (in blue) bands for $\lambda = 0$, $\varepsilon = \frac{1}{7}$, with \mathcal{F}_0 , so the effective operator is $v_F \sigma \cdot (-i\nabla) + \frac{1}{2}\varepsilon(-\Delta)$. We see that as we increase ν , additional spectral “pollution” arises, but their number stabilizes after some value of ν , for instance in the case of Figure 2, taking $\nu \geq 6$ does not change with respect to $\nu = 6$. The same phenomenon happens for other families \mathcal{F} , and at any value of ε .

Written differently, at ε fixed, when we increase ν we observe the spectral pollution as in Figure 2, due to the presence of the Laplace operator $-\Delta$. Moreover, at ν fixed, the spectral pollution disappears and the artificial bands are “expelled” as we decrease ε , as we can see on Figure 3.

In all the rest of the simulations, we will hence use $\nu = 2$, for any situation, it is a good compromise to obtain the sought-after bands, and small spectral pollution.

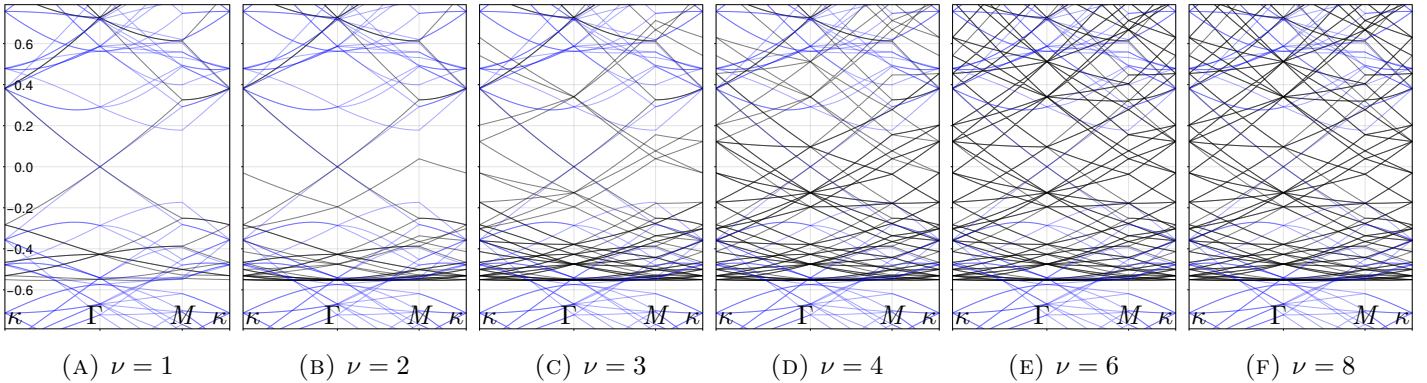


FIGURE 2. Letting ν vary at fixed $\varepsilon = \frac{1}{7}$, and $\mathcal{F} = \mathcal{F}_0$, $V = 0$.

5.3. Varying ℓ and k -dep. We take $\nu = 2$, $\varepsilon = \frac{1}{7}$. On Figure 4, we take $V = 0$, we let ℓ vary in $\{0, 1, 2\}$, and for $\ell \in \{1, 2\}$, we provide the band diagrams of the k -dependent families $\mathcal{F}_{\ell,k}$ and the ones of the k -independent families \mathcal{F}_ℓ . We also provide the result for the “6 states” family \mathcal{F}^6 defined in Section 4.7. It is natural to compare families having the same number of states, so we can focus on comparing \mathcal{F}_1 , $\mathcal{F}_{2,k}$ and \mathcal{F}^6 , which all have 6 states. We see that the other families than \mathcal{F}_0 reproduce the main branch better than \mathcal{F}_0 .

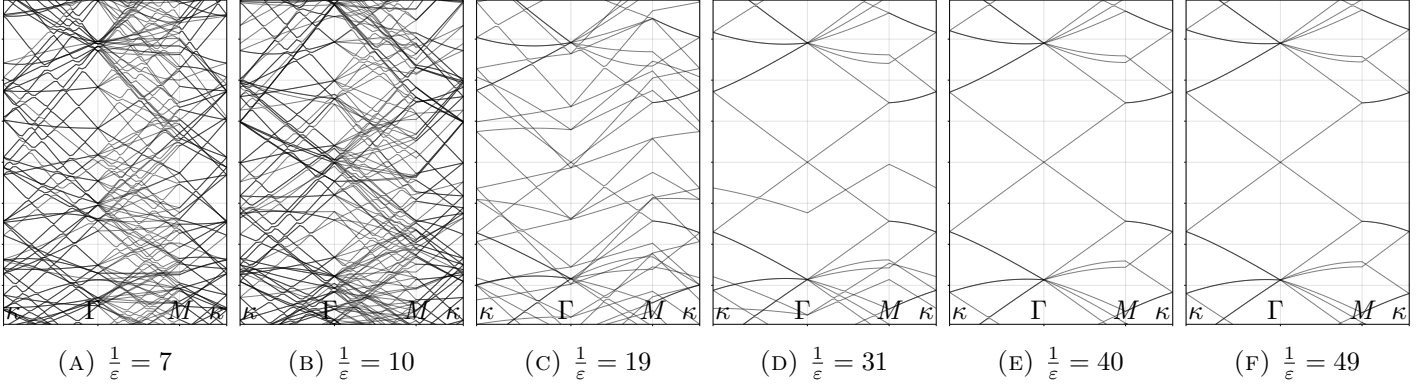


FIGURE 3. Letting ε decrease at fixed but large $\nu = 21$, and where only bands of the effective model are plotted. We chose \mathcal{F}_1 , $\nu = 21$, $V = 0$.

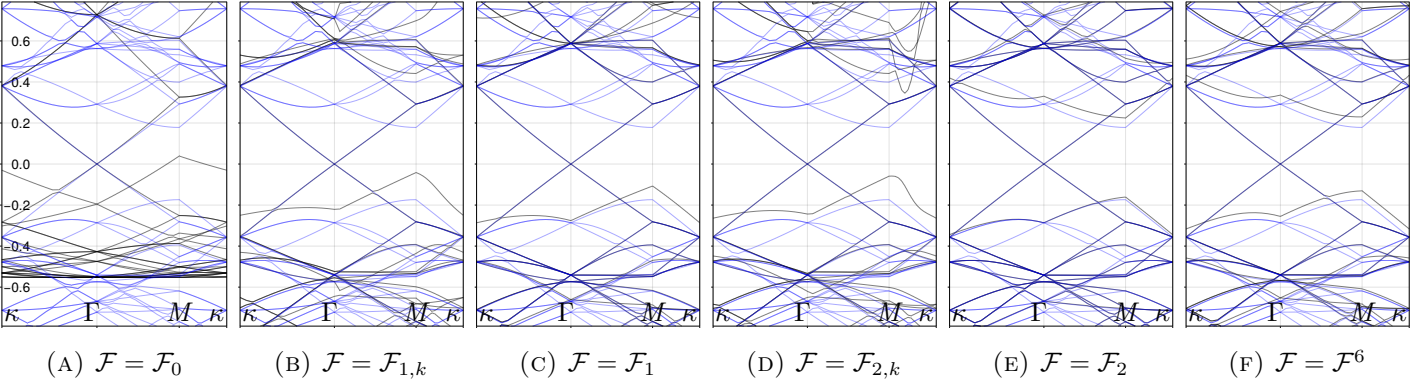


FIGURE 4. Letting ℓ vary, with $\varepsilon = \frac{1}{7}$, $\nu = 2$ and $V = 0$.

To better see the usefulness of the method, we also provide in Figure 5 the same band diagrams but with a potential $V = V_{\text{ng}}$ which does not have honeycomb symmetry. Let us define $\tilde{m}^1 := (1, 0)$, $\tilde{m}^2 := (0, 1)$, $\tilde{m}^3 := (0, 2)$. We used

$$V_{\text{ng}}(x) := 2\lambda \sum_{i=1}^3 \cos((\tilde{m}^i a^*) \cdot x). \quad (26)$$

Here again we see that the effective operator reproduces relatively well the exact bands.

5.4. Varying ε . Now let us take $V = V_{\text{honeycomb}}$ defined in (25), with $\lambda = 6$, \mathcal{F}_1 and $\nu = 2$, and let ε vary. On Figure 6, we display the band diagrams. The

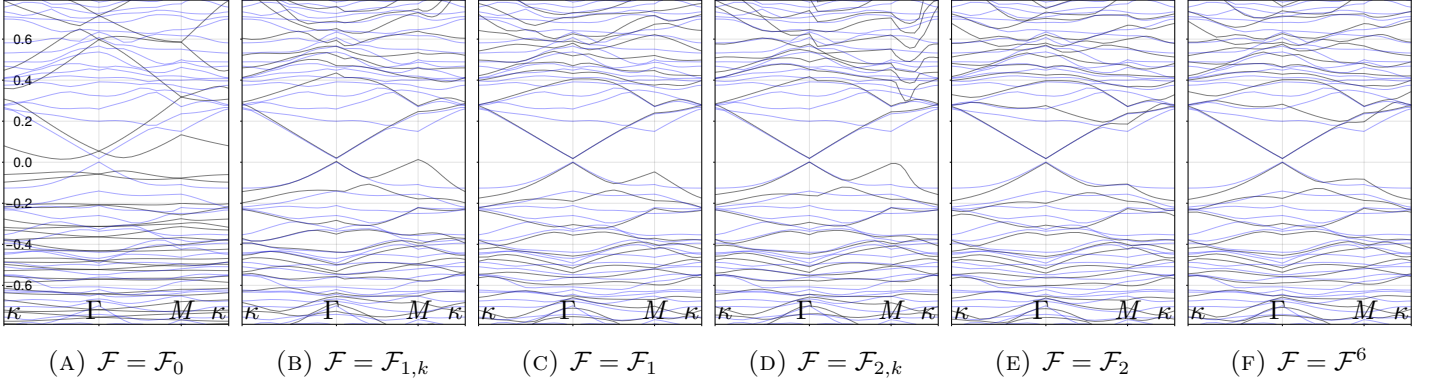


FIGURE 5. Letting ℓ vary, with $\varepsilon = \frac{1}{7}$, $\nu = 2$ and a non-zero $V = V_{\text{ng}}$ (with $\lambda = 5$) which does not have honeycomb symmetry, presented in (26).

bands are well reproduced and similarly as in Figure 3, the artificial bands are expelled as ε decreases.

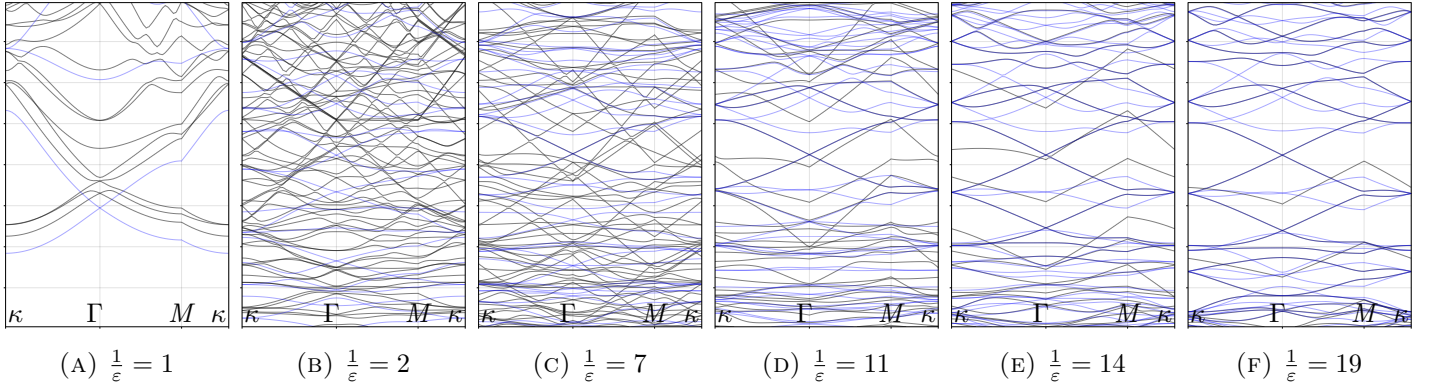


FIGURE 6. Letting ε vary, with \mathcal{F}_1 , $\nu = 2$, $V = V_{\text{honeycomb}}$ and $\lambda = 6$.

5.5. Varying λ . On Figure 7, we take $\varepsilon = \frac{1}{7}$, $\mathcal{F} = \mathcal{F}_1$, $V = V_{\text{honeycomb}}$, and we let λ vary, see (25). As expected, we observe that the branches coming from the Dirac cone progressively become inaccurate.

5.6. Asymptotics. We will use the relative distance

$$d(\psi, \phi) := \frac{\|\psi - \phi\|_{L^2_{\text{per}}(\Omega)}}{\frac{1}{2} \left(\|\psi\|_{L^2_{\text{per}}(\Omega)} + \|\phi\|_{L^2_{\text{per}}(\Omega)} \right)}.$$

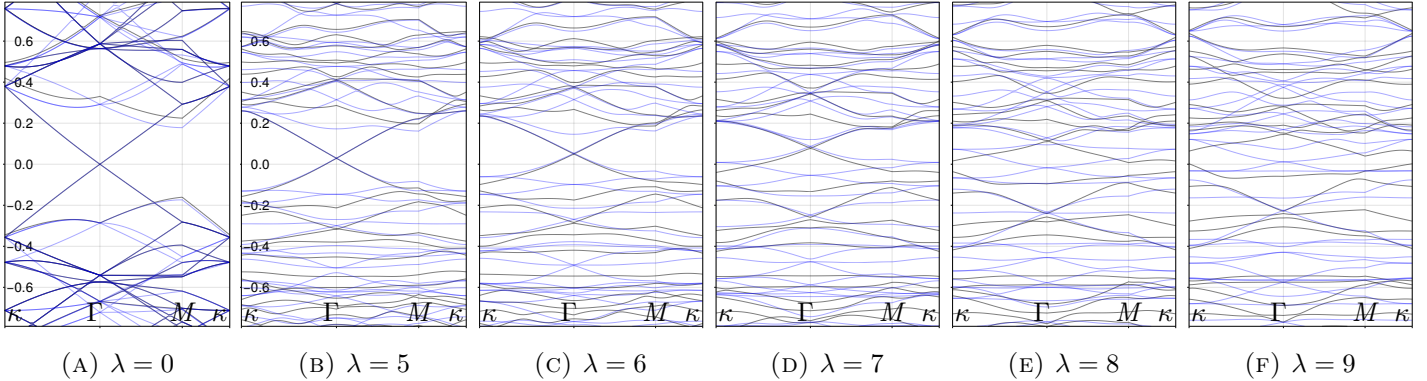


FIGURE 7. Letting λ vary, which is the coupling constant of V , with $V = V_{\text{honeycomb}}$, $\varepsilon = \frac{1}{7}$, $\nu = 2$ and $\mathcal{F} = \mathcal{F}_1$.

Since the eigenvectors w_1 and w_2 defined in (6) are exact when $k = 0$ and $V = 0$, we can consider that the two sources of error are the fact that $k \neq 0$ and $\lambda \neq 0$. Hence we want to better estimate the errors in k and λ , independently from each other. Thus on Figure 8, we represent

$$d(\Phi_k^\varepsilon, \mathcal{J}\alpha_k^\varepsilon), \quad (27)$$

in the two following cases.

- On the left, we take $\lambda = 0$, and $k = \mu K$ for instance, and we let $\mu \geq 0$ vary. Since $\lambda = 0$ then $V = 0$ and we only see the error coming from the fact that we are not at $k = 0$. As expected from variational perturbation theory, the error is proportional to $|\mu|^{\ell+1}$ for models of order ℓ (we precise that \mathcal{F}^6 is a model with order $\ell = 0$). Both for μ small and larger, the effective operator coming from perturbation theory (which is \mathcal{F}_1) is slightly more precise than the one coming from adding excited states in the variational space (which is \mathcal{F}^6). We can compare the results of those two operators because the corresponding families have the same number of microscopic states.
- On the right, we take $k = 0$ and let λ vary, so we only see the error coming from the fact that we are not at $V = 0$. Here, we see that for λ small enough, the effective operator built from first order perturbative vectors (\mathcal{F}_1) is slightly better than the effective operator coming from excited states (\mathcal{F}^6). However, this accuracy order is reversed for large V 's.

5.7. Conclusion. The goal of this document was to obtain accurate effective operators for the Bloch eigenmodes of the two-scales exact Schrödinger operator (1). The derivation of effective operators by using variational perturbation theory led to several models, depending on the perturbation order and on the momentum dependence.

Here are the main conclusions brought by the simulations.

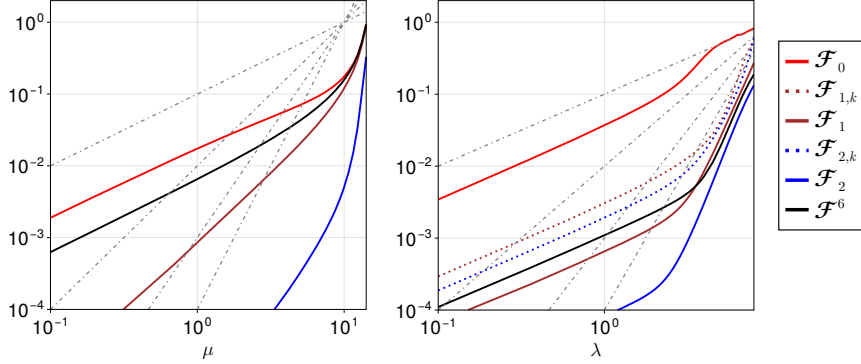


FIGURE 8. We take $V = V_{\text{honeycomb}}$, $\nu = 2$, $\frac{1}{\varepsilon} = 7$ and display the relative distance on eigenvectors (27) (between the exact and effective models). On the left, we take $\lambda = 0$ and let $k = \mu K$ vary on a one-dimensional segment starting from $k = 0$, we do not provide $\mathcal{F}_{\ell,k}$ and the curve of \mathcal{F}_2 is below the other ones and we do not see it. On the right we take $k = 0$ and we let λ (the intensity of V) vary. The grey lines are reference curves $(x/10)^a$ for $a \in \{1, 2, 3, 4\}$ to enable asymptotic behavior comparisons.

- The precision given by the massless Dirac operator can be significantly improved to approach the eigenmodes of the exact Bloch operator, as we saw on Figures 4 and 5;
- The cut-off ν needs to be well-chosen to avoid spectral pollution of the effective models. We can in general choose $\nu = 2$, as explained in Section 5.2;
- We are not retaining the k -dependent families $\mathcal{F}_{1,k}$ and $\mathcal{F}_{2,k}$ because of non-smooth behaviors and lack of accuracy seen in Figures 4, 5 and 8;
- As seen in Section 5.6, the effective operator \mathcal{F}_1 built with perturbative (with respect to the momentum) vectors at first order has most of the time better precision than the effective operator \mathcal{F}^6 coming from adding eigenstates at K , and hence we recover the same kind of conclusions as in [40, Section 6.3].

We believe that the use of the proposed effective operators could be of interest in some applications to model low-energy Dirac fermions, when precision is needed.

6. PROOF OF PROPOSITION 3.1

In this section, we derive the effective operator \mathbb{H}_k^ε written in (13) from the exact operator H_k^ε expressed in (10), by using the same method as in [21].

We define $a := \begin{pmatrix} a_1 \\ a_2 \end{pmatrix}$ and for $m \in \mathbb{Z}^2$, we will use the notation $ma := m_1 a_1 + m_2 a_2$. Our Fourier transform will be the operator $\mathbb{F} : L^2_{\text{per}}(\Omega) \rightarrow \ell^2(\mathbb{Z}^2)$

such that for any $f \in L^2_{\text{per}}(\Omega)$,

$$(\mathbb{F}f)_m = \widehat{f}_m = \frac{1}{\sqrt{|\Omega|}} \int_{\Omega} f(y) e^{-ima^*y} dy, \quad f(x) = \sum_{m \in \mathbb{Z}^2} \widehat{f}_m \frac{e^{ima^*x}}{\sqrt{|\Omega|}}. \quad (28)$$

The following result is classical and explains the decoupling between macroscopic and microscopic scales

Lemma 6.1. *Take $g \in C^\infty_{\text{per}}(\Omega)$ and $f \in L^2_{\text{per}}(\Omega)$. For any $N \in \mathbb{N} \cup \{0\}$ there is $c_N > 0$ such that uniformly in $\varepsilon \in]0, 1[\cap(1/\mathbb{N})$, we have*

$$\left| \int_{\Omega} g(x) f\left(\frac{x}{\varepsilon}\right) dx - |\Omega|^{-1} \int_{\Omega} g \int_{\Omega} f \right| \leq c_N \varepsilon^N. \quad (29)$$

Proof. Since $f \in L^2_{\text{per}}(\Omega)$ then $f \in L^1_{\text{per}}(\Omega)$ because Ω is bounded. We recall that $\varepsilon^{-1} \in \mathbb{N}$. We compute

$$\begin{aligned} \int_{\Omega} g(x) f\left(\frac{x}{\varepsilon}\right) dx &= |\Omega|^{-1} \sum_{n, m \in \mathbb{Z}^2} \widehat{g}_m \widehat{f}_n \int_{\Omega} e^{i(m + \frac{n}{\varepsilon})a^*x} dx = \sum_{n, m \in \mathbb{Z}^2} \widehat{g}_m \widehat{f}_n \delta_{m + \varepsilon^{-1}n} \\ &= \sum_{n \in \mathbb{Z}^2} \widehat{g}_{-\varepsilon^{-1}n} \widehat{f}_n = |\Omega|^{-1} \int_{\Omega} g \int_{\Omega} f + \sum_{n \in \mathbb{Z}^2 \setminus \{(0,0)\}} \widehat{g}_{-\varepsilon^{-1}n} \widehat{f}_n. \end{aligned}$$

Moreover,

$$\left| \sum_{n \in \mathbb{Z}^2 \setminus \{(0,0)\}} \widehat{g}_{-\varepsilon^{-1}n} \widehat{f}_n \right|^2 \leq \left(\sum_{n \in \mathbb{Z}^2 \setminus \{(0,0)\}} |\widehat{g}_{-\varepsilon^{-1}n}|^2 \right) \|f\|_{L^2_{\text{per}}(\Omega)}^2.$$

Since g is smooth, for any $N \in \mathbb{N}$, there exists $c_N > 0$ such that uniformly in $m \in \mathbb{Z}^2$, $|\widehat{g}_m| \leq \frac{c_N}{1+|m|^N}$, thus if $m \neq 0$, $|\widehat{g}_{-\varepsilon^{-1}m}| \leq \varepsilon^N \frac{c_N}{\varepsilon^N + |m|^N} \leq \varepsilon^N c_N |m|^{-N}$. \square

We will denote by $O(\varepsilon^\infty)$ any quantity X such that for any $N \in \mathbb{N}$, there exists $c_N > 0$ such that for any $\varepsilon \in]0, 1[\cap(1/\mathbb{N})$, $|X| \leq c_N \varepsilon^N$.

For any functions f and g and any $p, q \in \mathbb{R}^2$, we have

$$(-i\nabla_{p+q})(fg) = f(-i\nabla_p)g + g(-i\nabla_q)f. \quad (30)$$

From (30) and $\nabla_{\varepsilon^{-1}K}Q = \varepsilon^{-1}Q\nabla_K$ we deduce that

$$\begin{aligned} (-i\nabla_{\varepsilon^{-1}K+k} + A)(g(x)\varphi\left(\frac{x}{\varepsilon}\right)) \\ = \varphi\left(\frac{x}{\varepsilon}\right) ((-i\nabla_k + A)g)(x) + \varepsilon^{-1}g(x) (-i\nabla_K\varphi)\left(\frac{x}{\varepsilon}\right), \end{aligned}$$

and thus

$$\begin{aligned} (-i\nabla_{\varepsilon^{-1}K+k} + A)^2(g(x)\varphi\left(\frac{x}{\varepsilon}\right)) &= \varphi\left(\frac{x}{\varepsilon}\right) ((-i\nabla_k + A)^2g)(x) \\ &\quad + 2\varepsilon^{-1}((-i\nabla_k + A)g)(x) \cdot (-i\nabla_K\varphi)\left(\frac{x}{\varepsilon}\right) + \varepsilon^{-2}g(x) ((-i\nabla_K)^2\varphi)\left(\frac{x}{\varepsilon}\right). \end{aligned}$$

This enables to make the computation

$$\begin{aligned} H_k^\varepsilon(g(x)\varphi\left(\frac{x}{\varepsilon}\right)) &= g(x) ((h_K - E_F)\varphi)\left(\frac{x}{\varepsilon}\right) \\ &\quad + \varphi\left(\frac{x}{\varepsilon}\right) \left(\frac{1}{2}\varepsilon^2(-i\nabla_k + A)^2 + \varepsilon V\right)g(x) \\ &\quad + \varepsilon((-i\nabla_k + A)g)(x) \cdot (-i\nabla_K\varphi)\left(\frac{x}{\varepsilon}\right). \end{aligned}$$

We proceed by taking Ω -periodic functions f, g, ξ, φ and computing

$$\begin{aligned}
& \varepsilon^{-1} |\Omega| \langle fQ\xi, H_k^\varepsilon gQ\varphi \rangle_{L^2_{\text{per}}(\Omega)} \\
&= \varepsilon^{-1} |\Omega| \int_{\Omega} (\bar{f}g)(x) (\bar{\xi}(h_K - E_F)\varphi)\left(\frac{x}{\varepsilon}\right) dx \\
&\quad + |\Omega| \int_{\Omega} (\bar{f}((-i\nabla_k + A)g))(x) \cdot (\bar{\xi}(-i\nabla_K\varphi))\left(\frac{x}{\varepsilon}\right) dx \\
&\quad + |\Omega| \int_{\Omega} (\bar{f}(\frac{1}{2}\varepsilon(-i\nabla_k + A)^2 + V)g)(x) (\bar{\xi}\varphi)\left(\frac{x}{\varepsilon}\right) dx \\
&\stackrel{(29)}{=} \varepsilon^{-1} \langle f, g \rangle \langle \xi, (h_K - E_F)\varphi \rangle + \langle f, (-i\nabla_k + A)g \rangle \cdot \langle \xi, -i\nabla_K\varphi \rangle \\
&\quad + \langle f, (\frac{1}{2}\varepsilon(-i\nabla_k + A)^2 + V)g \rangle \langle \xi, \varphi \rangle + O(\varepsilon^\infty).
\end{aligned}$$

Then we take $\xi = \psi_a$, $f = \alpha_a$ and $\varphi = \psi_b$, $g = \beta_b$, which concludes the proof of Proposition 3.1.

7. COMPUTATION OF MATRIX COEFFICIENTS USING GRAPHENE SYMMETRIES

In this section, our goal is to compute scalar products of the kind

$$\begin{aligned}
\langle Y_1 w_a, Y_2(-i\partial_{K,j})w_b \rangle, & \quad \langle Y_1(-i\partial_{K,n})w_a, Y_2(-i\partial_{K,j})w_b \rangle, \\
& \quad \langle Y_1(-i\partial_{K,q})w_a, Y_2(-i\partial_{K,j})Y_3(-i\partial_{K,m})w_b \rangle,
\end{aligned}$$

with respectively one, two or three derivatives, for particular operators Y_j 's of interest involved in graphene. This will provide the tools to compute all the matrices involved in (15), by using symmetries. See [83] for a systematic study of this kind of quantities.

7.1. One derivative. The case of one derivative is well-known [35], [21, (S3)]. If $R_{\frac{2\pi}{3}}m = ym$ with $m \in \mathbb{C}^2$, then

$$m = \begin{cases} t \begin{pmatrix} 1 \\ -\eta i \end{pmatrix} & \text{if } y = \omega^\eta \text{ and } \eta \in \{-1, 1\}, \text{ for some } t \in \mathbb{C}, \\ 0 & \text{otherwise,} \end{cases} \quad (31)$$

and this leads to the computation of $\langle w_a, (-i\nabla_K)w_b \rangle$ for instance, see (16). Here we recall the computation when only one derivative is involved. As in [21], we define

$$(\mathfrak{R}f)(x_1, x_2) := f(x_1, -x_2).$$

We will use the spaces of pseudo-periodic functions

$$L_k^2(\Omega) := \left\{ f \in H_{\text{loc}}^1(\mathbb{R}^2) \mid f(x + ma) = e^{ik \cdot (ma)} f(x), \forall m \in \mathbb{Z}^2 \right\}.$$

We set the conjugation $S_j := e^{iKx} Y_j e^{-iKx}$ for $j \in \{1, 2\}$, as operators of $L_K^2(\Omega)$.

Lemma 7.1 (One derivative). *Take two bounded operators Y_1 and Y_2 of $L_{\text{per}}^2(\Omega)$, such that S_1 and S_2 commute with $\mathcal{R}_{\frac{2\pi}{3}}$ and with \mathcal{CP} .*

- There exist $v \in \mathbb{C}$ such that for any $j, a \in \{1, 2\}$, $\langle Y_1 w_a, Y_2(-i\partial_{K,j})w_a \rangle = 0$ and

$$\langle Y_1 w_1, Y_2(-i\nabla_K)w_2 \rangle = v \begin{pmatrix} 1 \\ -i \end{pmatrix}, \quad \langle Y_1 w_2, Y_2(-i\nabla_K)w_1 \rangle = \bar{v} \begin{pmatrix} 1 \\ i \end{pmatrix}.$$

- Take $\iota_a \in \{-1, 1\}$ for any $a \in \{1, 2\}$ and assume that for any $a \in \{1, 2\}$, $S_a \mathfrak{R} = \iota_a \mathfrak{R} S_a$. Then $v \in \mathbb{R}$ if $\iota_1 \iota_2 = 1$ and $v \in i\mathbb{R}$ if $\iota_1 \iota_2 = -1$.

Proof. We recall that

$$\partial_{K,n} e^{-iKx} = e^{-iKx} \partial_n. \quad (32)$$

so

$$\langle Y_1 w_a, Y_2(-i\partial_{K,j})w_b \rangle = -i \langle S_1 \phi_a, S_2 \partial_j \phi_b \rangle. \quad (33)$$

We will prove the equivalent statements on those last quantities. We recall that

$$\mathcal{R}_\theta \nabla = R_{-\theta} \nabla \mathcal{R}_\theta. \quad (34)$$

We define the vectors $m^{(ab)} \in \mathbb{C}^2$ by $m_j^{(ab)} := \langle S_1 \phi_a, S_2 \partial_j \phi_b \rangle$. We have

$$\begin{aligned} m^{(ab)} &= \langle S_1 \phi_a, S_2 \nabla \phi_b \rangle = \left\langle \mathcal{R}_{\frac{2\pi}{3}} S_1 \phi_a, \mathcal{R}_{\frac{2\pi}{3}} S_2 \nabla \phi_b \right\rangle = \left\langle S_1 \mathcal{R}_{\frac{2\pi}{3}} \phi_a, S_2 \mathcal{R}_{\frac{2\pi}{3}} \nabla \phi_b \right\rangle \\ &\stackrel{(34)}{=} R_{-\frac{2\pi}{3}} \left\langle S_1 \mathcal{R}_{\frac{2\pi}{3}} \phi_a, \nabla S_2 \mathcal{R}_{\frac{2\pi}{3}} \phi_b \right\rangle \stackrel{(8)}{=} \omega^{b-a} R_{-\frac{2\pi}{3}} m^{(ab)}. \end{aligned}$$

Thus $R_{\frac{2\pi}{3}} m^{(ab)} = \omega^{b-a} m^{(ab)}$. The only vector invariant under $R_{\frac{2\pi}{3}}$ is 0 so $m^{(11)} = m^{(22)} = 0$. Then $R_{\frac{2\pi}{3}} m^{(12)} = \omega m^{(12)}$ implies $m^{(12)} \in \text{Ker}(R_{\frac{2\pi}{3}} - \omega) = \mathbb{C} \begin{pmatrix} 1 \\ -i \end{pmatrix}$ so $m^{(12)} = \nu \begin{pmatrix} 1 \\ -i \end{pmatrix}$ for some $\nu \in \mathbb{C}$. Similarly, $m^{(21)} = g \begin{pmatrix} 1 \\ i \end{pmatrix}$ for some $g \in \mathbb{C}$. We define $\underline{1} := 2$ and $\underline{2} := 1$ and will use

$$\mathcal{P}\mathcal{C}\nabla = -\nabla\mathcal{P}\mathcal{C}, \quad \mathcal{P}\mathcal{C}\phi_a = \phi_{\underline{a}}.$$

We have

$$\begin{aligned} \nu &= m_1^{(12)} = \langle S_1 \phi_1, S_2 \partial_1 \phi_2 \rangle = \langle \mathcal{P}\mathcal{C} S_2 \partial_1 \phi_2, \mathcal{P}\mathcal{C} S_1 \phi_1 \rangle = \langle S_2 \mathcal{P}\mathcal{C} \partial_1 \phi_2, S_1 \mathcal{P}\mathcal{C} \phi_1 \rangle \\ &= -\langle S_2 \partial_1 \mathcal{P}\mathcal{C} \phi_2, S_1 \mathcal{P}\mathcal{C} \phi_1 \rangle = -\langle S_2 \partial_1 \phi_1, S_1 \phi_2 \rangle = -\overline{\langle S_1 \phi_2, S_2 \partial_1 \phi_1 \rangle} \\ &= -\overline{m_1^{(21)}} = -\bar{g}. \end{aligned}$$

In [21, Appendix 1] it is proved that

$$\mathfrak{R}\phi_1 = (-1)^\eta \phi_2 \quad (35)$$

with $\eta \in \{\pm 1\}$. We use $Y_a \mathfrak{R} = \iota_a \mathfrak{R} Y_a$ and moreover we have

$$\mathfrak{R}\partial_n = (-1)^{n+1} \partial_n \mathfrak{R}, \quad (36)$$

also written $\mathfrak{R}\nabla = \sigma_3 \nabla \mathfrak{R}$. We compute

$$\begin{aligned} \nu &= m_1^{(12)} = \langle S_1 \phi_1, S_2 \partial_1 \phi_2 \rangle = \langle \mathfrak{R} S_1 \phi_1, \mathfrak{R} S_2 \partial_1 \phi_2 \rangle = \iota_1 \iota_2 \langle S_1 \mathfrak{R} \phi_1, S_2 \mathfrak{R} \partial_1 \phi_2 \rangle \\ &\stackrel{(36)}{=} \iota_1 \iota_2 \langle S_1 \mathfrak{R} \phi_1, S_2 \partial_1 \mathfrak{R} \phi_2 \rangle \stackrel{(35)}{=} \iota_1 \iota_2 \langle S_1 \phi_2, S_2 \partial_1 \phi_1 \rangle = \iota_1 \iota_2 m_1^{(21)} = -\iota_1 \iota_2 \bar{\nu}. \end{aligned}$$

Hence $\nu \in i\mathbb{R}$ if $\iota_1 \iota_2 = 1$ and $\nu \in \mathbb{R}$ if $\iota_1 \iota_2 = -1$. We have $\langle S_1 w_1, S_2 \nabla w_2 \rangle = \nu \begin{pmatrix} 1 \\ -i \end{pmatrix}$ and $\langle S_1 w_2, S_2 \nabla w_1 \rangle = -\bar{\nu} \begin{pmatrix} 1 \\ i \end{pmatrix}$ so we deduce the conclusion using (33) and $v = -i\nu$. \square

7.2. **Two derivatives.** We define

$$D := \begin{pmatrix} 1 & i \\ i & -1 \end{pmatrix} = \sigma_3 + i\sigma_1.$$

We start by showing the following result.

Lemma 7.2. *Take $M \in \mathbb{C}^{2 \times 2}$ and $y \in \{1, \omega, \bar{\omega}\}$. Then $R_{\frac{2\pi}{3}}MR_{-\frac{2\pi}{3}} = yM$ if and only if*

$$M = \begin{cases} s\mathbb{1}_2 + r\sigma_2 & \text{if } y = 1, \text{ for some } s, r \in \mathbb{C} \\ sD & \text{if } y = \omega, \text{ for some } s \in \mathbb{C} \\ sD^* & \text{if } y = \bar{\omega}, \text{ for some } s \in \mathbb{C}. \end{cases}$$

Proof. We write $M = \begin{pmatrix} a & b \\ c & d \end{pmatrix}$, and compute

$$\begin{aligned} 0 &= 4 \left(R_{\frac{2\pi}{3}}MR_{-\frac{2\pi}{3}} - yM \right) \\ &= \begin{pmatrix} a(1-4y) + 3d + \sqrt{3}(c+b) & b(1-4y) - 3c + \sqrt{3}(d-a) \\ c(1-4y) - 3b + \sqrt{3}(d-a) & d(1-4y) + 3a - \sqrt{3}(b+c) \end{pmatrix}. \end{aligned} \quad (37)$$

When $y = 1$, the system is equivalent to

$$\begin{cases} c + b = \sqrt{3}(a - d) \\ \sqrt{3}(c + b) = a - d \end{cases}$$

itself equivalent to $d = a$ and $c = -b$. When $y = \omega = -\frac{1}{2} + i\frac{\sqrt{3}}{2}$, (37) is equivalent to

$$\begin{cases} \sqrt{3}(a+d) + c + b - 2ia = 0 \\ \sqrt{3}(b-c) + d - a - 2ib = 0 \\ \sqrt{3}(c-b) + d - a - 2ic = 0 \\ \sqrt{3}(d+a) - b - c - 2id = 0. \end{cases}$$

Adding the first and last equations gives $a = -d$, subtracting the second one and the third one gives $b = c$, and finally the first equation gives $b = ia$.

When $y = \bar{\omega}$, we replace i by $-i$ in the previous system, we obtain $a = -d$, $b = c$ and $b = -ia$. \square

The last lemma enables to obtain the form of the matrix elements involving two derivatives, as shown by the next result.

Lemma 7.3 (Two derivatives). *Take two bounded operators Y_1 and Y_2 of $L^2_{\text{per}}(\Omega)$, such that S_1 and S_2 commute with $\mathcal{R}_{\frac{2\pi}{3}}$ and with \mathcal{CP} .*

- *There exist $t, s, r \in \mathbb{C}$ such that for any $n, j \in \{1, 2\}$,*

$$\begin{aligned} \langle Y_1(-i\partial_{K,n})w_1, Y_2(-i\partial_{K,j})w_2 \rangle &= rD_{nj} \\ \langle Y_1(-i\partial_{K,n})w_2, Y_2(-i\partial_{K,j})w_1 \rangle &= \bar{r}D_{nj}^* \\ \langle Y_1(-i\partial_{K,n})w_1, Y_2(-i\partial_{K,j})w_1 \rangle &= t\delta_{nj} + s(\sigma_2)_{nj} \\ \langle Y_1(-i\partial_{K,n})w_2, Y_2(-i\partial_{K,j})w_2 \rangle &= \bar{t}\delta_{nj} - \bar{s}(\sigma_2)_{nj}. \end{aligned} \quad (38)$$

- *Take $\iota_a \in \{-1, 1\}$ for any $a \in \{1, 2\}$ and assume that for any $a \in \{1, 2\}$, $S_a\mathfrak{R} = \iota_a\mathfrak{R}S_a$. Then $t, s \in \mathbb{R}$. Moreover, $r \in \mathbb{R}$ if $\iota_1\iota_2 = 1$ and $r \in i\mathbb{R}$ if $\iota_1\iota_2 = -1$.*

Proof. From (32) we have

$$\langle Y_1(-i\partial_{K,n})w_a, Y_2(-i\partial_{K,j})w_b \rangle = \langle S_1\partial_n\phi_a, S_2\partial_j\phi_b \rangle.$$

We define the 2×2 matrices $M^{(ab)}$ by

$$M_{ij}^{(ab)} := \langle S_1\partial_i\phi_a, S_2\partial_j\phi_b \rangle.$$

We recall that for any $A \in \mathcal{M}_{2 \times 2}(\mathbb{C})$, $C_1, C_2 \in \mathcal{M}_{2 \times 1}(\mathbb{C})$ and $L_1, L_2 \in \mathcal{M}_{1 \times 2}(\mathbb{C})$, we have $A \begin{pmatrix} C_1 & C_2 \end{pmatrix} = (AC_1 \quad AC_2)$ and $\begin{pmatrix} L_1 \\ L_2 \end{pmatrix} A = \begin{pmatrix} L_1 A \\ L_2 A \end{pmatrix}$. Moreover, we consider $\nabla = \begin{pmatrix} \partial_1 \\ \partial_2 \end{pmatrix}$ as a column vector and $\nabla^T = (\partial_1 \quad \partial_2)$. Hence

$$\begin{aligned} R_{\frac{2\pi}{3}} M^{(ab)} &= R_{\frac{2\pi}{3}} \left(\langle S_1\nabla\phi_a, S_2\partial_1\phi_b \rangle \quad \langle S_1\nabla\phi_a, S_2\partial_2\phi_b \rangle \right) \\ &= \left(\left\langle R_{\frac{2\pi}{3}} S_1\nabla\phi_a, S_2\partial_1\phi_b \right\rangle \quad \left\langle R_{\frac{2\pi}{3}} S_1\nabla\phi_a, S_2\partial_2\phi_b \right\rangle \right) \\ &= \left\langle R_{\frac{2\pi}{3}} S_1\nabla\phi_a, S_2\nabla^T\phi_b \right\rangle \end{aligned}$$

and

$$\begin{aligned} M^{(ab)} R_{-\frac{2\pi}{3}} &= \begin{pmatrix} \langle S_1\partial_1\phi_a, S_2\nabla\phi_b \rangle^T \\ \langle S_1\partial_2\phi_a, S_2\nabla\phi_b \rangle^T \end{pmatrix} R_{-\frac{2\pi}{3}} = \begin{pmatrix} \langle S_1\partial_1\phi_a, S_2\nabla\phi_b \rangle^T R_{\frac{2\pi}{3}}^T \\ \langle S_1\partial_2\phi_a, S_2\nabla\phi_b \rangle^T R_{\frac{2\pi}{3}}^T \end{pmatrix} \\ &= \begin{pmatrix} \left\langle S_1\partial_1\phi_a, R_{\frac{2\pi}{3}} S_2\nabla\phi_b \right\rangle^T \\ \left\langle S_1\partial_2\phi_a, R_{\frac{2\pi}{3}} S_2\nabla\phi_b \right\rangle^T \end{pmatrix} = \left\langle S_1\nabla\phi_a, S_2 \left(R_{\frac{2\pi}{3}} \nabla \right)^T \phi_b \right\rangle. \end{aligned}$$

We deduce that

$$\begin{aligned} \left(R_{\frac{2\pi}{3}} M^{(ab)} R_{-\frac{2\pi}{3}} \right)_{ij} &= \left(\left\langle S_1 R_{\frac{2\pi}{3}} \nabla\phi_a, S_2 \left(R_{\frac{2\pi}{3}} \nabla \right)^T \phi_b \right\rangle \right)_{ij} \\ &= \left\langle \left(S_1 R_{\frac{2\pi}{3}} \nabla\phi_a \right)_i, \left(S_2 R_{\frac{2\pi}{3}} \nabla\phi_b \right)_j \right\rangle \\ &= \left\langle \mathcal{R}_{\frac{2\pi}{3}} \left(S_1 R_{\frac{2\pi}{3}} \nabla\phi_a \right)_i, \mathcal{R}_{\frac{2\pi}{3}} \left(S_2 R_{\frac{2\pi}{3}} \nabla\phi_b \right)_j \right\rangle \\ &\stackrel{(34)}{=} \left\langle \left(S_1 \nabla \mathcal{R}_{\frac{2\pi}{3}} \phi_a \right)_i, \left(S_2 \nabla \mathcal{R}_{\frac{2\pi}{3}} \phi_b \right)_j \right\rangle \\ &\stackrel{(8)}{=} \omega^{b-a} \left\langle (S_1 \nabla\phi_a)_i, (S_2 \nabla\phi_b)_j \right\rangle \\ &= \omega^{b-a} \langle S_1\partial_i\phi_a, S_2\partial_j\phi_b \rangle = \omega^{b-a} M_{ij}^{(ab)}, \end{aligned}$$

so $R_{\frac{2\pi}{3}} M^{(ab)} R_{-\frac{2\pi}{3}} = \omega^{b-a} M^{(ab)}$. Using Lemma 7.2, we obtain that there exist $r, r', t, s, t', s' \in \mathbb{C}$ such that

$$\begin{aligned} \langle S_1\partial_n\phi_1, S_2\partial_j\phi_2 \rangle &= r D_{nj} \\ \langle S_1\partial_n\phi_2, S_2\partial_j\phi_1 \rangle &= r' D_{nj}^* \\ \langle S_1\partial_n\phi_1, S_2\partial_j\phi_1 \rangle &= t \delta_{nj} + s (\sigma_2)_{nj} \\ \langle S_1\partial_n\phi_2, S_2\partial_j\phi_2 \rangle &= t' \delta_{nj} + s' (\sigma_2)_{nj}. \end{aligned}$$

Then

$$\begin{aligned} M_{nm}^{(ab)} &= \langle S_1 \partial_n \phi_a, S_2 \partial_m \phi_b \rangle = \overline{\langle \mathcal{P}C S_1 \partial_n \phi_a, \mathcal{P}C S_2 \partial_m \phi_b \rangle} \\ &= \overline{\langle S_1 \partial_n \mathcal{P}C \phi_a, S_2 \partial_m \mathcal{P}C \phi_b \rangle} = \overline{\langle S_1 \partial_n \phi_{\underline{a}}, S_2 \partial_m \phi_{\underline{b}} \rangle} = \overline{M_{nm}^{(ab)}}, \end{aligned} \quad (39)$$

hence

$$\begin{aligned} t &= M_{11}^{(11)} = \overline{M_{11}^{(22)}} = \bar{t}' \\ is &= M_{21}^{(11)} = \overline{M_{21}^{(22)}} = \overline{is'} = -i \bar{s}' \\ r &= M_{11}^{(12)} = \overline{M_{11}^{(21)}} = \bar{r}'. \end{aligned} \quad (40)$$

This concludes the proof of (38).

$$\begin{aligned} M_{nm}^{(ab)} &= \langle S_1 \partial_n \phi_a, S_2 \partial_m \phi_b \rangle = \langle \mathfrak{R} S_1 \partial_n \phi_a, \mathfrak{R} S_2 \partial_m \phi_b \rangle \\ &= \iota_a \iota_b \langle S_1 \mathfrak{R} \partial_n \phi_a, S_2 \mathfrak{R} \partial_m \phi_b \rangle \stackrel{(36)}{=} \iota_a \iota_b (-1)^{n+m} \langle S_1 \partial_n \mathfrak{R} \phi_a, S_2 \partial_m \mathfrak{R} \phi_b \rangle \\ &\stackrel{(35)}{=} \iota_a \iota_b (-1)^{n+m} (-1)^{2\eta} \langle S_1 \partial_n \phi_{\underline{a}}, S_2 \partial_m \phi_{\underline{b}} \rangle = \iota_a \iota_b (-1)^{n+m} M_{nm}^{(ab)}. \end{aligned} \quad (41)$$

Finally,

$$\begin{aligned} t &= M_{11}^{(11)} = M_{11}^{(22)} = t' = \bar{t} \\ is &= M_{12}^{(11)} = -M_{12}^{(22)} = -is' = i\bar{s} \\ r &= M_{11}^{(12)} = \iota_1 \iota_2 M_{11}^{(21)} = \iota_1 \iota_2 r' = \iota_1 \iota_2 \bar{r}'. \end{aligned}$$

This enables us to conclude that $t, s \in \mathbb{R}$ and that $r \in \mathbb{R}$ if $\iota_1 \iota_2 = 1$ and $r \in i\mathbb{R}$ if $\iota_1 \iota_2 = -1$. \square

As a consequence of Lemma 7.3, when the assumptions are satisfied we can compute

$$\langle Y_1 D_k w_a, Y_2 D_k w_a \rangle_{a \in \{1,2\}} = t, \quad \langle Y_1 D_k w_1, Y_2 D_k w_2 \rangle = r e^{i2\theta_k}. \quad (42)$$

Indeed, using that $k_1 = |k| \cos \theta_k$, $k_2 = |k| \sin \theta_k$, we have

$$\begin{aligned} \langle Y_1 D_k w_1, Y_2 D_k w_2 \rangle &= \frac{r}{|k|^2} (k_1^2 - k_2^2 + 2ik_1 k_2) = \frac{r}{|k|^2} (k_1 + ik_2)^2 \\ &= \frac{r}{|k|^2} (k_{\mathbb{C}})^2 = r e^{i2\theta_k}. \end{aligned}$$

7.3. Three derivatives. To finish, we compute the elements involving three derivatives.

Let us define

$$F_{qjm}^{ab} := \langle Y_1(-i\partial_{K,q})w_a, Y_2(-i\partial_{K,j})Y_3(-i\partial_{K,m})w_b \rangle,$$

and

$$\chi_1 := F_{111}^{11}, \quad \chi_2 := -iF_{222}^{11}, \quad \gamma_1 := F_{122}^{12}, \quad \gamma_2 := F_{212}^{12}, \quad \gamma_3 := F_{221}^{12}.$$

For any proposition \mathbb{P} , we define $\delta_{\mathbb{P}} := 1$ if \mathbb{P} is true and $\delta_{\mathbb{P}} := 0$ otherwise.

Lemma 7.4 (Three derivatives). *Assume that the bounded operators Y_1, Y_2, Y_3 of $L^2_{\text{per}}(\Omega)$ commute with $\mathcal{R}_{\frac{2\pi}{3}}$, \mathcal{CP} and \mathfrak{A} . Then*

$$\begin{aligned} F_{122}^{11} &= F_{212}^{11} = F_{221}^{11} = F_{122}^{22} = F_{212}^{22} = F_{221}^{22} = -F_{111}^{11} = -F_{111}^{22} = -\chi_1 \in \mathbb{R} \\ F_{112}^{11} &= F_{211}^{11} = F_{121}^{11} = -F_{112}^{22} = -F_{211}^{22} = -F_{121}^{22} = -F_{222}^{11} = F_{222}^{22} = -i\chi_2 \in i\mathbb{R}, \end{aligned} \quad (43)$$

and

$$\begin{aligned} F_{122}^{12} &= F_{122}^{21} = iF_{211}^{12} = -iF_{211}^{21} = \gamma_1 \in \mathbb{R} \\ F_{212}^{12} &= F_{212}^{21} = iF_{121}^{12} = -iF_{121}^{21} = \gamma_2 \in \mathbb{R} \\ F_{221}^{12} &= F_{221}^{21} = iF_{112}^{12} = -iF_{112}^{21} = \gamma_3 \in \mathbb{R} \\ F_{111}^{12} &= F_{111}^{21} = iF_{222}^{12} = -iF_{222}^{21} = \gamma_1 + \gamma_2 + \gamma_3 \in \mathbb{R}. \end{aligned} \quad (44)$$

If moreover $Y_1 = Y_3$ and $Y_2 = 1$, then $\chi_2 = 0$ and $\gamma_1 = \gamma_3$.

Proof. Using \mathcal{PC} and \mathfrak{A} , the same arguments as in (39) and (41) show that for any $a, b, q, j, m \in \{1, 2\}$,

$$F_{qjm}^{ab} = \overline{F_{qjm}^{ab}}, \quad F_{qjm}^{ab} = (-1)^{q+j+m+1} F_{qjm}^{ab},$$

where we used that $(-1)^{\delta_{q-2} + \delta_{j-2} + \delta_{m-2}} = (-1)^{q+j+m+1}$, which comes from the commutation of \mathfrak{A} with ∂_s for $s \in \{q, j, m\}$. Using both equations we deduce that $F_{qjm}^{ab} = (-1)^{q+j+m+1} \overline{F_{qjm}^{ab}}$ hence

$$\begin{aligned} F_{qjm}^{ab} &= F_{qjm}^{ab} \in \mathbb{R} & \text{if } q+j+m \in 2\mathbb{N}+1, \\ F_{qjm}^{ab} &= -F_{qjm}^{ab} \in i\mathbb{R} & \text{if } q+j+m \in 2\mathbb{N}. \end{aligned} \quad (45)$$

For $q \in \{1, 2\}$, let us denote by $P_q : \mathbb{C}^2 \rightarrow \mathbb{C}$ the projection on the q^{th} coordinate, and $Q := 2R_{-\frac{2\pi}{3}} = \begin{pmatrix} -1 & \sqrt{3} \\ -\sqrt{3} & -1 \end{pmatrix}$. As previously we set $S_j := e^{iKx} Y_j e^{-iKx}$ for $j \in \{1, 2\}$. We have

$$\begin{aligned} &8\omega^{a-b} F_{qjm}^{ab} \\ &= 8\omega^{a-b} \langle S_1(-i\partial_q)\phi_a, S_2(-i\partial_j)S_3(-i\partial_m)\phi_b \rangle \\ &= 8\omega^{a-b} \langle S_1(P_q(-i\nabla))\phi_a, S_2(P_j(-i\nabla))S_3(P_m(-i\nabla))\phi_b \rangle \\ &= 8\omega^{a-b} \left\langle \mathcal{R}_{\frac{2\pi}{3}} S_1(P_q(-i\nabla))\phi_a, \mathcal{R}_{\frac{2\pi}{3}} S_2(P_j(-i\nabla))S_3(P_m(-i\nabla))\phi_b \right\rangle \\ &\stackrel{(34)}{=} 8\omega^{a-b} \times \\ &\left\langle S_1(P_q R_{-\frac{2\pi}{3}}(-i\nabla)) \mathcal{R}_{\frac{2\pi}{3}} \phi_a, S_2(P_j R_{-\frac{2\pi}{3}}(-i\nabla)) S_3(P_m R_{-\frac{2\pi}{3}}(-i\nabla)) \mathcal{R}_{\frac{2\pi}{3}} \phi_b \right\rangle \\ &\stackrel{(8)}{=} \sum_{1 \leq q', j', m' \leq 2} \langle S_1 Q_{qq'}(-i\partial_{q'})\phi_a, S_2 Q_{jj'}(-i\partial_{j'}) S_3 Q_{mm'}(-i\partial_{m'})\phi_b \rangle \\ &= \sum_{1 \leq q', j', m' \leq 2} Q_{qq'} Q_{jj'} Q_{mm'} F_{q'j'm'}^{ab} \end{aligned} \quad (46)$$

We then define the coordinates

$$\begin{aligned} g_1 &:= (1, 1, 1), & g_2 &:= (1, 1, 2), & g_3 &:= (1, 2, 1), & g_4 &:= (1, 2, 2), \\ g_5 &:= (2, 1, 1), & g_6 &:= (2, 1, 2), & g_7 &:= (2, 2, 1), & g_8 &:= (2, 2, 2), \end{aligned}$$

the vectors $F^{ab} \in \mathbb{C}^8$ by $F^{ab} := \left(F_{g_\mu}^{ab} \right)_{1 \leq \mu \leq 8}$, and the 8×8 matrix W by

$$W_{\alpha\beta} := Q_{(g_\alpha)_1(g_\beta)_1} Q_{(g_\alpha)_2(g_\beta)_2} Q_{(g_\alpha)_3(g_\beta)_3},$$

where $(g_\alpha)_q$ is the q^{th} coordinate of g_α , where $q \in \{1, 2, 3\}$ and $\alpha, \beta \in \{1, \dots, 8\}$. We can compute

$$W = \begin{pmatrix} -1 & \sqrt{3} & \sqrt{3} & -3 & \sqrt{3} & -3 & -3 & 3\sqrt{3} \\ -\sqrt{3} & -1 & 3 & \sqrt{3} & 3 & \sqrt{3} & -3\sqrt{3} & -3 \\ -\sqrt{3} & 3 & -1 & \sqrt{3} & 3 & -3\sqrt{3} & \sqrt{3} & -3 \\ -3 & -\sqrt{3} & -\sqrt{3} & -1 & 3\sqrt{3} & 3 & 3 & \sqrt{3} \\ -\sqrt{3} & 3 & 3 & -3\sqrt{3} & -1 & \sqrt{3} & \sqrt{3} & -3 \\ -3 & -\sqrt{3} & 3\sqrt{3} & 3 & -\sqrt{3} & -1 & 3 & \sqrt{3} \\ -3 & 3\sqrt{3} & -\sqrt{3} & 3 & -\sqrt{3} & 3 & -1 & \sqrt{3} \\ -3\sqrt{3} & -3 & -3 & -\sqrt{3} & -3 & -\sqrt{3} & -\sqrt{3} & -1 \end{pmatrix},$$

the relation (46) can be written, for any $a, b \in \{1, 2\}$,

$$\left(W - 8\omega^{a-b} \right) F^{ab} = 0. \quad (47)$$

Let us first determine F^{11} and F^{22} . We define

$$A := \begin{pmatrix} \sqrt{3} & -9 & -3 & -3\sqrt{3} & 3 & -\sqrt{3} & \sqrt{3} & 3 \\ 3 & \sqrt{3} & 3\sqrt{3} & -9 & -\sqrt{3} & 3 & -3 & -\sqrt{3} \\ -24 & 0 & 0 & 24 & 0 & 24 & 24 & 0 \\ 0 & 24 & 24 & 0 & 24 & 0 & 0 & -24 \\ 0 & -6 & 6 & 0 & 0 & -2\sqrt{3} & 2\sqrt{3} & 0 \\ -6 & 0 & 0 & -6 & -2\sqrt{3} & 0 & 0 & -2\sqrt{3} \\ 2\sqrt{3} & 0 & 0 & 2\sqrt{3} & -6 & 0 & 0 & -6 \\ 0 & 2\sqrt{3} & -2\sqrt{3} & 0 & 0 & -6 & 6 & 0 \end{pmatrix}$$

respecting $\det A \neq 0$, and

$$\tilde{A} := \begin{pmatrix} 0 & 1 & 0 & 0 & -1 & 0 & 0 & 0 \\ 0 & 0 & 0 & 1 & 0 & -1 & 0 & 0 \\ 0 & 0 & 0 & 0 & 0 & 0 & 0 & 0 \\ 0 & 0 & 0 & 0 & 0 & 0 & 0 & 0 \\ 0 & 1 & -1 & 0 & 0 & 0 & 0 & 0 \\ 1 & 0 & 0 & 1 & 0 & 0 & 0 & 0 \\ 0 & 0 & 0 & 0 & 1 & 0 & 0 & 1 \\ 0 & 0 & 0 & 0 & 0 & 1 & -1 & 0 \end{pmatrix}$$

and we can check that $A(W - 8) = 96\tilde{A}$. Thus the systems (47) with $a = b$ can be rewritten $\tilde{A}F^{11} = 0$ and $\tilde{A}F^{22} = 0$. The first system is equivalent to

$$F_{112}^{11} = F_{211}^{11} = F_{121}^{11} = -F_{222}^{11}, \quad \text{and} \quad F_{122}^{11} = F_{212}^{11} = F_{221}^{11} = -F_{111}^{11}. \quad (48)$$

Using (45) we have $F_{222}^{11} \in i\mathbb{R}$ so $\chi_2 = -iF_{222}^{11} \in \mathbb{R}$. Similarly, we have $\chi_1 \in \mathbb{R}$. Again using (45), we deduce (43).

We now determine F^{12} and F^{21} . We define

$B :=$

$$\begin{pmatrix} 7\sqrt{3} - 3i & -3 - 3\sqrt{3}i & 0 & 0 & -3 + \sqrt{3}i & \sqrt{3} + 3i & 4\sqrt{3} & 0 \\ -3 + \sqrt{3}i & -3\sqrt{3} + 3i & 0 & 0 & \sqrt{3} + 3i & 3 - \sqrt{3}i & 4\sqrt{3}i & 0 \\ -\sqrt{3} - 3i & -3 - 3\sqrt{3}i & 0 & 0 & -3 + \sqrt{3}i & -7\sqrt{3} + 3i & 4\sqrt{3} & 0 \\ -3 + \sqrt{3}i & 5\sqrt{3} + 3i & 0 & 0 & -7\sqrt{3} + 3i & 3 - \sqrt{3}i & 4\sqrt{3}i & 0 \\ -4\sqrt{3} & 12 & 0 & 0 & 4\sqrt{3}i & -4\sqrt{3} & -4\sqrt{3} + 12i & 0 \\ -8\sqrt{3}i & -8\sqrt{3} & 0 & 0 & 0 & 0 & -8\sqrt{3}i & -8\sqrt{3} \\ 24\sqrt{3} & 0 & 0 & 24\sqrt{3} & -24\sqrt{3}i & 0 & 0 & -24\sqrt{3}i \\ 0 & 24\sqrt{3} & -24\sqrt{3} & 0 & 0 & -24\sqrt{3}i & 24\sqrt{3} & 0 \end{pmatrix}$$

respecting $\det B \neq 0$, and

$$\tilde{B} := \begin{pmatrix} -i & 0 & 0 & 0 & 0 & 0 & 0 & 1 \\ 0 & i & 0 & 0 & 0 & 0 & 1 & 0 \\ 0 & 0 & -1 & 0 & 0 & i & 0 & 0 \\ 0 & 0 & 0 & 1 & i & 0 & 0 & 0 \\ 0 & 0 & 0 & 0 & 1 & i & i & -1 \\ 0 & 0 & 0 & 0 & 0 & 0 & 0 & 0 \\ 0 & 0 & 0 & 0 & 0 & 0 & 0 & 0 \\ 0 & 0 & 0 & 0 & 0 & 0 & 0 & 0 \end{pmatrix}.$$

We can check that $B(W - 8\omega) = 96\tilde{B}$, so the system (47) with $a \neq b$ can be rewritten $\tilde{B}F^{21} = 0$, and we deduce that

$$\begin{aligned} F_{222}^{21} &= iF_{111}^{21}, & F_{221}^{21} &= -iF_{112}^{21}, & F_{212}^{21} &= -iF_{121}^{21} \\ F_{211}^{21} &= iF_{122}^{21} & F_{211}^{21} + iF_{212}^{21} + iF_{221}^{21} - F_{222}^{21} &= 0, \end{aligned}$$

and we can conclude by using (45).

If moreover, $Y_1 = Y_3$ and $Y_2 = 1$, then

$$\begin{aligned} -i\chi_2 &= F_{121}^{11} = \langle Y_1(-i\partial_{K,1})w_1, (-i\partial_{K,2})Y_1(-i\partial_{K,1})w_1 \rangle \\ &= \langle (-i\partial_{K,2})Y_1(-i\partial_{K,1})w_1, Y_1(-i\partial_{K,1})w_1 \rangle \\ &= \overline{\langle Y_1(-i\partial_{K,1})w_1, (-i\partial_{K,2})Y_1(-i\partial_{K,1})w_1 \rangle} = \overline{F_{121}^{11}} = i\chi_2, \end{aligned}$$

so $\chi_2 = 0$. Similarly,

$$\begin{aligned} \gamma_3 &= F_{221}^{12} = \langle Y_1(-i\partial_{K,2})w_1, (-i\partial_{K,2})Y_1(-i\partial_{K,1})w_2 \rangle \\ &= \overline{\langle Y_1(-i\partial_{K,1})w_2, (-i\partial_{K,2})Y_1(-i\partial_{K,2})w_1 \rangle} = \overline{F_{122}^{21}} = \overline{\gamma_1} = \gamma_1. \end{aligned}$$

□

7.4. Computation of the matrices (15) in the case of $\mathcal{F}_{1,k}$, proof of Proposition 4.1. Those computations involve one or two derivatives, so Lemma 7.3 is going to provide the answers.

7.4.1. *Satisfying the assumptions of Lemma 7.3.* We define $h := \frac{1}{2}(-\Delta) + v$ as an operator of $L_K^2(\Omega)$. With the notation (7), we define the operator \mathcal{P} as the orthogonal projection of $L_K^2(\Omega)$ onto $\text{Span}(\phi_1, \phi_2) \subset L_K^2(\Omega)$, and the pseudo-inverse

$$Z := \begin{cases} \left((E_{\mathbb{F}} - h)|_{\mathcal{P}_{\perp}L_K^2(\Omega) \rightarrow \mathcal{P}_{\perp}L_K^2(\Omega)} \right)^{-1} & \text{on } \mathcal{P}_{\perp}L_K^2(\Omega) \\ 0 & \text{on } \mathcal{P}L_K^2(\Omega). \end{cases}$$

We have formally $Z = e^{iKx} R e^{-iKx}$, and Z has the role of “ S_a ” in Lemma 7.3. We have that

$$\sigma_3(ma) = m_1\sigma_3a_1 + m_2\sigma_3a_2 = -m_1a_2 - m_2a_1 = -(\sigma_1m)a$$

so

$$K \cdot (-(\sigma_1m)a) = -K \cdot (\sigma_3(ma)) = -(\sigma_3K) \cdot ma \stackrel{\sigma_3K = -K}{=} K \cdot ma.$$

If $\phi \in L_K^2(\Omega)$, then

$$\begin{aligned} (\mathfrak{A}\phi)(x + ma) &= \phi(\sigma_3(x + ma)) = \phi(\sigma_3x - (-(\sigma_1m)a)) \\ &= e^{iK \cdot (-(\sigma_1m)a)} \phi(\sigma_3x) = e^{iK \cdot ma} (\mathfrak{A}\phi)(x), \end{aligned}$$

and $\mathfrak{R}\phi \in L_K^2(\Omega)$. Hence \mathfrak{R} sends $L_K^2(\Omega)$ into itself. Moreover, since $\mathfrak{R}\phi_1 = (-1)^\eta \phi_2$, then \mathfrak{R} sends $\mathcal{P}L_K^2(\Omega)$ into itself and $\mathcal{P}_\perp L_K^2(\Omega)$ as well. We have $\mathfrak{R}\Delta = \Delta\mathfrak{R}$ and by the symmetries (4), $\mathfrak{R}v = v\mathfrak{R}$ so \mathfrak{R} commutes with h . We can conclude that

$$\mathfrak{R}Z = Z\mathfrak{R},$$

and we are going to be able to satisfy the assumption “ $S_a\mathfrak{R} = \mathfrak{R}S_a$ ” of Lemma 7.3.

Moreover, $R_{\frac{2\pi}{3}}K - K$ belongs to the reciprocal lattice of \mathbb{L} so for any $m \in \mathbb{Z}^2$, $K \cdot R_{-\frac{2\pi}{3}}(ma) = R_{\frac{2\pi}{3}}K \cdot (ma) = K \cdot ma$ modulo 2π , and we can see that $\mathcal{R}_{\frac{2\pi}{3}}$ sends $L_K^2(\Omega)$ onto itself and commutes with Z . Similarly $\mathcal{P}\mathcal{C}$ sends $L_K^2(\Omega)$ onto itself and commutes with Z .

We proved that all the assumptions of Lemma 7.3 are satisfied, with $\iota_1\iota_2 = 1$, so we can apply it.

7.4.2. *Matrix S.* We have $S = (\langle RD_k w_a, RD_k w_b \rangle)_{1 \leq a, b \leq 2}$. Applying Lemma 7.3 and (42) yields S as in (20).

7.4.3. *Matrix M.* We have

$$\begin{aligned} M_{ab} &= \langle R(-i\partial_{K,\alpha})w_a, (h_K - E_F)R(-i\partial_{K,\beta})w_b \rangle \\ &= -\langle (-i\partial_{K,\alpha})w_a, R(-i\partial_{K,\beta})w_b \rangle, \end{aligned}$$

and we proceed as for S .

7.4.4. *Matrix T.* Then

$$T_{ab} = \langle w_a, (-i\nabla_K)RD_k w_b \rangle = |k|^{-1} \sum_{1 \leq \alpha \leq 2} k_\alpha \langle w_a, (-i\nabla_K)R(-i\partial_{K,\alpha})w_b \rangle.$$

Using Lemma 7.3,

$$\begin{aligned} T_{11} &= |k|^{-1} (k_1 \langle w_1, (-i\nabla_K)R(-i\partial_{K,1})w_1 \rangle + k_2 \langle w_1, (-i\nabla_K)R(-i\partial_{K,2})w_1 \rangle) \\ &= |k|^{-1} \left(k_1 \begin{pmatrix} t' \\ i s' \end{pmatrix} + k_2 \begin{pmatrix} -i s' \\ t' \end{pmatrix} \right) = |k|^{-1} \begin{pmatrix} k_1 t' - i k_2 s' \\ i k_1 s' + k_2 t' \end{pmatrix} \\ &= (t' \mathbf{1} - s' \sigma_2) \frac{k}{|k|}. \end{aligned}$$

Similarly,

$$T_{12} = r' e^{i\theta_k} \begin{pmatrix} 1 \\ i \end{pmatrix}, \quad T_{21} = r' e^{-i\theta_k} \begin{pmatrix} 1 \\ -i \end{pmatrix}, \quad T_{22} = (t' \mathbf{1} + s' \sigma_2) \frac{k}{|k|}$$

so we have (21).

7.4.5. *Matrix L.* The matrix L is the first one which involves three derivatives in the scalar products. We apply Lemma 7.4, we are in the configuration where “ $Y_1 = Y_3$ ” and “ $Y_2 = 1$ ” so $\chi_2 = 0$ and $\gamma_1 = \gamma_3$. We define $e_1 := \begin{pmatrix} 1 \\ 0 \end{pmatrix}$ and $e_2 := \begin{pmatrix} 0 \\ 1 \end{pmatrix}$. We have $F_{qjm}^{11} = \chi(-1)^{1+\delta_{q=j=m}} \delta_{q+j+m \in 2\mathbb{N}+1}$. We compute, for $a \in \{1, 2\}$,

$$\begin{aligned} \langle \psi_{a+2}, (-i\nabla)\psi_{a+2} \rangle &= \langle RD_k w_a, (-i\nabla_K)RD_k w_a \rangle \\ &= |k|^{-2} \sum_{1 \leq q, j, m \leq 2} e_j k_q k_m F_{qjm}^{aa} = \chi |k|^{-2} \begin{pmatrix} k_1^2 - k_2^2 \\ -2k_1 k_2 \end{pmatrix} = \chi \begin{pmatrix} \cos(2\theta_k) \\ -\sin(2\theta_k) \end{pmatrix}. \end{aligned}$$

and

$$\begin{aligned}
\langle \psi_3, (-i\nabla)\psi_4 \rangle &= \langle RD_k w_1, (-i\nabla_K)RD_k w_2 \rangle \\
&= |k|^{-2} \begin{pmatrix} k_1^2(2\gamma_1 + \gamma_2) + k_2^2\gamma_2 - 2ik_1k_2\gamma_1 \\ -ik_1^2\gamma_2 - ik_2^2(2\gamma_1 + \gamma_2) + 2k_1k_2\gamma_1 \end{pmatrix} \\
&= \begin{pmatrix} \gamma_2 + 2\gamma_1 e^{-i\theta_k} \cos \theta_k \\ -i\gamma_2 + 2\gamma_1 e^{-i\theta_k} \sin \theta_k \end{pmatrix} = \overline{\langle \psi_4, (-i\nabla)\psi_3 \rangle}
\end{aligned}$$

and we can conclude (22).

7.5. Case of excited states, proof of Proposition 4.3. From [35], defining $\phi_3(x) := e^{iK \cdot x} w_3(x)$, we have that $\mathcal{R}_{\frac{2\pi}{3}} \phi_3 = \mathcal{PC} \phi_3 = (-1)^\eta \mathfrak{A} \phi_3 = \phi_3$ and

$$R_{\frac{2\pi}{3}} \langle \phi_1, (-i\nabla)\phi_3 \rangle = R_{\frac{2\pi}{3}} \left\langle \mathcal{R}_{\frac{2\pi}{3}} \phi_1, \mathcal{R}_{\frac{2\pi}{3}} (-i\nabla)\phi_3 \right\rangle \stackrel{(34)}{=} \bar{\omega} \langle \phi_1, (-i\nabla)\phi_3 \rangle.$$

Thus using also (31), $\langle \phi_1, (-i\nabla)\phi_3 \rangle = i\tilde{v}_F \begin{pmatrix} 1 \\ i \end{pmatrix}$ for some $\tilde{v}_F \in \mathbb{C}$. Similarly, $\langle \phi_2, (-i\nabla)\phi_3 \rangle = ic \begin{pmatrix} 1 \\ -i \end{pmatrix}$ for some $c \in \mathbb{C}$, and $\langle \phi_3, (-i\nabla)\phi_3 \rangle = 0$. Then

$$\langle \phi_1, (-i\nabla)\phi_3 \rangle = \overline{\langle \mathcal{PC} \phi_1, \mathcal{PC} (-i\nabla)\phi_3 \rangle} = \overline{\langle \phi_2, (-i\nabla)\mathcal{PC} \phi_3 \rangle} = \overline{\langle \phi_2, (-i\nabla)\phi_3 \rangle}$$

and we deduce that $\tilde{v}_F = -\bar{c}$. Moreover,

$$\begin{aligned}
\langle \phi_1, (-i\nabla)\phi_3 \rangle &= \langle \mathfrak{A} \phi_1, \mathfrak{A} (-i\nabla)\phi_3 \rangle = -\sigma_3 (-1)^\eta \langle \phi_2, (-i\nabla)\mathfrak{A} \phi_3 \rangle \\
&= -\sigma_3 \langle \phi_2, (-i\nabla)\phi_3 \rangle
\end{aligned}$$

implying that $\tilde{v}_F = -c$ and $\tilde{v}_F \in \mathbb{R}$.

8. FORMAL DERIVATION OF THE PERTURBATION SERIES FOR THE MACROSCOPIC FUNCTIONS

In this section, we provide a formal justification of the choice of adding derivatives with respect to the momentum, in the families \mathcal{F} of Section 4.2.

We recall that when $A = 0$, from (9) we have

$$h_q^\varepsilon = \frac{1}{2}(-i\nabla_q)^2 + v(x) + \varepsilon V(\varepsilon x).$$

We formally define $X = \varepsilon x$ as the macroscopic spatial variable, and hence $\nabla = \nabla_x + \varepsilon \nabla_X$, $\nabla_q = \nabla_{x,q} + \varepsilon \nabla_X$ where $\nabla_{x,q} := \nabla_x + iq$, and

$$\begin{aligned}
h_q^\varepsilon &= \frac{1}{2} \left((-i\nabla_{x,q})^2 + 2\varepsilon(-i\nabla_{x,q})(-i\nabla_X) + \varepsilon^2(-i\nabla_X)^2 \right) + v(x) + \varepsilon V(X) \\
&= h_q + \varepsilon(-i\nabla_{x,q})(-i\nabla_X) + \frac{1}{2}\varepsilon^2(-i\nabla_X)^2 + \varepsilon V(X).
\end{aligned}$$

We are interested in a branch $\varepsilon \mapsto (E_q^\varepsilon, U_q^\varepsilon)$ of eigenmodes of h_q^ε . Thus we expand the eigenmodes in ε as

$$\xi_q^\varepsilon(x, X) = \xi_q^0(x, X) + \varepsilon \xi_q^1(x, X) + O(\varepsilon^2), \quad E_q^\varepsilon = E_q^0 + \varepsilon E_q^1 + O(\varepsilon^2).$$

Since ξ_q^ε is $\varepsilon^{-1}\Omega$ -periodic, then the ξ_q^j 's as well, for $j \in \{0, 1\}$. The zeroth order in ε of $h_q^\varepsilon \xi_q^\varepsilon = E_q^\varepsilon \xi_q^\varepsilon$ is

$$\left(\frac{1}{2}(-i\nabla_{x,q})^2 + v(x) - E_q^0 \right) \xi_q^0(x, X) = 0 \tag{49}$$

and the following order is

$$\begin{aligned} & \left(\frac{1}{2}(-i\nabla_{x,q})^2 + v(x) - E^0\right) \xi_q^1(x, X) \\ &= - \left((-i\nabla_{x,q}) \cdot (-i\nabla_X) + V(X) - E^1\right) \xi_q^0(x, X). \end{aligned} \quad (50)$$

From (49) we obtain that for q in a neighborhood of K , there exist Ω -periodic functions α_q^1, α_q^2 such that

$$\xi_q^0(x, X) = \sum_{a=1}^2 \alpha_q^a(X) g_q^a(x),$$

where $(g_q^a)_{1 \leq a \leq 2}$ are the Bloch eigenfunction of $\frac{1}{2}(-i\nabla_q)^2 + v$ at the Fermi level. Then (50) becomes

$$\begin{aligned} & \left(\frac{1}{2}(-i\nabla_{x,p})^2 + v(x) - E^0\right) \xi_q^1(x, X) \\ &= - \sum_{j=1}^2 \left((-i\nabla_X \alpha_q^j)(X) \cdot (-i\nabla_{x,q} g_q^j)(x) + (V(X) - E_q^1) \alpha_q^j(X) g_q^j(x)\right). \end{aligned}$$

This equation has a solution if and only if the right-hand side of this last equation is orthogonal to $\text{Span}(g_q^a)_{a \in \{1,2\}}$, that is, for all $X \in \Omega$,

$$0 = \sum_{j=1}^2 (-i\nabla_X \alpha_q^j)(X) \cdot \langle g_q^a, (-i\nabla_{x,q} g_q^j) \rangle_{L^2_{\text{per}}(\Omega)} + (V(X) - E_q^1) \alpha_q^j(X) \delta_{aj}.$$

By using that $\langle g_q^a, g_q^b \rangle = \delta_{ab}$, it is equivalent to

$$(\mathcal{D}_q - E_q^1) \alpha_q = 0,$$

where $F_q := (\langle g_q^a, (-i\nabla_{x,q} g_q^b) \rangle)_{1 \leq a, b \leq 2}$ and

$$\mathcal{D}_q := F_q \cdot (-i\nabla_X) + \mathbf{1}_{2 \times 2} \otimes V(X).$$

Finally, we are interested in $q = K + \varepsilon k$ so we can expand

$$g_{K+\varepsilon k}^b = g_K^b + \varepsilon \left(\delta_K^+ g^b\right)(k) + O(\varepsilon^2) = w_b + \varepsilon \left(\delta_K^+ g^b\right)(k) + O(\varepsilon^2),$$

where $(\delta_x^+ f) y$ is the directional derivative of a function f at x in direction y . We now expand

$$\xi_q^0(x, X) = \sum_{a=1}^2 \alpha_q^a(X) \left(w_a + \varepsilon (\delta_K^+ g^a)(k)\right) + O(\varepsilon^2)$$

Let us denote by $P_{\mathcal{F}}$ the orthogonal projection onto the subspace (12). The error between the exact and the approximate eigenfunctions is bounded (up to a constant independent of ε) by $\|P_{\mathcal{F}}^\perp \xi_q^\varepsilon\|$, see [40]. We focus on the first order error in ε . In the case where $\mathcal{F} = \mathcal{F}^0$, we have

$$\left\| P_{\mathcal{F}^0}^\perp \xi_q^\varepsilon \right\|_{L^2_{\text{per}}(\Omega)} \leq \varepsilon \left\| P_{\mathcal{F}^0}^\perp \left(\xi_q^1 + \sum_{a=1}^2 \alpha_q^a (\delta_K^+ g^a)(k) \right) \right\|_{L^2_{\text{per}}(\Omega)} + O(\varepsilon^2)$$

while in the case where $\mathcal{F} = \mathcal{F}^1$, since $(\delta_K^+ g^a)(k) \in \text{Span } \mathcal{F}^1$ we have that $P_{\mathcal{F}^1}^\perp (\delta_K^+ g^a)(k) = 0$ and

$$\left\| P_{\mathcal{F}^1}^\perp \xi_q^\varepsilon \right\|_{L_{\text{per}}^2(\Omega)} \leq \varepsilon \left\| P_{\mathcal{F}^1}^\perp \xi_q^1 \right\|_{L_{\text{per}}^2(\Omega)} + O(\varepsilon^2).$$

Moreover, since $\mathcal{F}^0 \subset \mathcal{F}^1$, we have that for any function f , $\|P_{\mathcal{F}^1}^\perp f\|_{L_{\text{per}}^2(\Omega)} \leq \|P_{\mathcal{F}^0}^\perp f\|_{L_{\text{per}}^2(\Omega)}$. We see that taking a family containing the first derivatives cuts the term $(\delta_K^+ g^a)(k)$ and leads to expect that the effective operator will be more accurate.

RESEARCH DATA MANAGEMENT

The Julia [13] code enabling to produce the figures of this document can be found on the Github repository

https://github.com/lgarrigue/superlattice_graphene

ACKNOWLEDGEMENT

I thank Eric Cancès for a useful discussion.

APPENDIX A. FORMAL DEGENERATE PERTURBATION THEORY

Here we review first order degenerate perturbation theory when the degeneracy is lifted at first order and when the degeneracy is exactly 2. We are only interested in the formal computations and will not be precise about the rigorous assumptions that are needed, see for instance [50] in [77] for this purpose.

A.1. The problem. Consider some self-adjoint operators A^0, A^1, A^2 of a Hilbert space \mathcal{H} . Take, for any $s \in \mathbb{R}$, a Hamiltonian

$$A(s) = A^0 + sA^1 + s^2A^2$$

and assume that there exists an eigenvalue $E^0 \in \mathbb{R}$ of A^0 such that $\dim \text{Ker}(A^0 - E^0) = 2$. Then there exists two branch eigenstates $s \mapsto U_n(s) \in \mathcal{H}$ of $A(s)$ for $n \in \{-, +\}$, analytic in $s \in [0, s_0[$ for some $s_0 > 0$, such that $\text{Ker}(A^0 - E^0) = \text{Span}(U_-(0), U_+(0))$. The corresponding eigenvalues are denoted by $E_n(s)$. We expand in the so-called Rayleigh-Schrödinger series

$$U_n(s) = U_n^0 + sU_n^1 + s^2U_n^2 + O(s^3), \quad E_n(s) = E_n^0 + sE_n^1 + s^2E_n^2 + O(s^3).$$

The goal is to compute U_n^0 and U_n^1 when the degeneracy is lifted at first order. This problem is well-known in the physics literature, see for instance [47, 50]. We provide the computations here for completeness.

A.2. The reasoning. We consider intermediate normalization, hence $U_n^k \perp U_n^0$ for any $k \in \mathbb{N} \setminus \{0\}$, but we do not necessarily have $\|U_n(s)\| = 1$, see [40, Appendix A] for more details on this procedure. Nevertheless, as presented in [40, Lemma C.1], perturbation vectors from intermediate normalization are equal to perturbation vectors from unit normalization at zeroth and first order, so the conclusion will not change.

We develop at the first 3 orders the eigenvalue equations

$$(A(s) - E_n(s))U_n(s) = 0$$

and obtain

$$(A^0 - E^0)U_n^0 = 0, \quad (51)$$

$$(A^1 - E_n^1)U_n^0 + (A^0 - E^0)U_n^1 = 0, \quad (52)$$

$$(A^2 - E_n^2)U_n^0 + (A^1 - E_n^1)U_n^1 + (A^0 - E^0)U_n^2 = 0. \quad (53)$$

Let us denote by P the orthogonal projection onto $\text{Ker}(A^0 - E^0)$, and $P_\perp := 1 - P$. Let us define the pseudoinverse

$$G := \begin{cases} \left((E^0 - A^0)|_{P_\perp \mathcal{H} \rightarrow P_\perp \mathcal{H}} \right)^{-1} & \text{on } P_\perp \mathcal{H} \\ 0 & \text{on } P\mathcal{H}, \end{cases}$$

extended by linearity on \mathcal{H} . Applying G to (52) yields

$$P_\perp U_n^1 = G(A^1 - E_n^1)U_n^0 = GA^1 U_n^0, \quad (54)$$

while applying P gives

$$PA^1 P U_n^0 = E_n^1 U_n^0,$$

that is (E_n^1, U_n^0) is an eigenmode of the matrix $PA^1 P$, in a basis we are free to choose, this is how we get E_n^1 . Then we define $P_n^1 := P(1 - \tilde{P}_n^1)$ where \tilde{P}_n^1 is the orthogonal projection onto $\text{Ker}(P(A^1 - E_n^1)P|_{P\mathcal{H}}) \subset P\mathcal{H}$, hence P_n^1 is the orthogonal projection onto $P\mathcal{H} \cap (\text{Ker}(P(A^1 - E_n^1)P))^\perp$. For any vector $u \in \mathcal{H}$, let us denote by P_u the orthogonal projection onto $\text{Span } u$. We assume that degeneracies are lifted at first order, i.e. that $(PA^1 P)|_{P\mathcal{H} \rightarrow P\mathcal{H}}$ has no degenerate eigenvalue, then we have $P_n^1 = P_{U_{-n}^0}$. We apply P_n^1 to (53) and obtain

$$\begin{aligned} 0 &= P_n^1(A^1 - E_n^1)U_n^1 + P_n^1 A^2 U_n^0 \\ &\stackrel{P+P_\perp=1}{=} P_n^1(A^1 - E_n^1)P U_n^1 + P_n^1(A^1 - E_n^1)P_\perp U_n^1 + P_n^1 A^2 U_n^0 \\ &\stackrel{P U_n^1 = P_n^1 U_n^1}{=} P_n^1(A^1 - E_n^1)P_n^1 U_n^1 + P_n^1 A^1 P_\perp U_n^1 + P_n^1 A^2 U_n^0 \\ &\stackrel{(54)}{=} P_n^1(A^1 - E_n^1)P_n^1 U_n^1 + P_n^1 A^1 G A^1 U_n^0 + P_n^1 A^2 U_n^0 \\ &= -P_n^1(E_n^1 - A^1)P_n^1 U_n^1 + P_n^1(A^2 + A^1 G A^1)U_n^0, \end{aligned}$$

where we used that $U_n^1 \perp U_n^0$ hence $P U_n^1 = P_n^1 U_n^1$. Finally, degeneracy is lifted at first order so the restriction $(P_n^1(E_n^1 - A^1)P_n^1)|_{\text{Span } U_{-n}^0 \rightarrow \text{Span } U_{-n}^0}$ is invertible and its inverse is $(E_n^1 - E_{-n}^1)^{-1} P_{U_{-n}^0}$. We apply this operator in the last equation, yielding

$$\begin{aligned} P U_n^1 &= (E_n^1 - E_{-n}^1)^{-1} P_{U_{-n}^0} (A^2 + A^1 G A^1) U_n^0 \\ &= \frac{\langle U_{-n}^0, (A^2 + A^1 G A^1) U_n^0 \rangle}{E_n^1 - E_{-n}^1} U_{-n}^0. \end{aligned} \quad (55)$$

A.3. **Conclusion.** To conclude, we saw that U_n^0 are vectors which diagonalize the matrix PA^1P , i.e. such that

$$PA^1PU_n^0 = E_n^1U_n^0.$$

Then assembling (54) and (55), we can deduce the first order

$$U_n^1 = GA^1U_n^0 + \frac{\langle U_{-n}^0, (A^2 + A^1GA^1)U_n^0 \rangle}{E_n^1 - E_{-n}^1}U_{-n}^0. \quad (56)$$

Using the scalar products of (52) and (53) against U_n^0 , we also obtain

$$\begin{aligned} E_n^1 &= \langle U_n^0, A^1U_n^0 \rangle, \\ E_n^2 &= \langle U_n^0, A^2U_n^0 \rangle + \langle U_n^0, A^1U_n^1 \rangle = \langle U_n^0, (A^2 + A^1GA^1)U_n^0 \rangle \end{aligned}$$

APPENDIX B. DEGENERATE PERTURBATION THEORY FOR OUR PROBLEM

B.1. **Directional derivatives.** We recall the definition of directional derivatives. Let us take two open normed spaces B and C , and a map $f : B \rightarrow C$. We consider $x, y \in B$ such that there exists $s_0 > 0$ with $x + sy \in B$ uniformly in $s \in [0, s_0[$. If the limit

$$(\delta_x^+ f)(y) := \lim_{s \rightarrow 0^+} \frac{f(x + sy) - f(x)}{s}$$

exists, then we say that this is the directional derivative of f in the direction y . Similarly, we can define the directional derivatives of order ℓ of f at x in the direction y as $(\delta_x^{+, \ell} f)(y) := \left(\frac{d^\ell}{ds^\ell} \varphi_y \right) \Big|_{s=0}$, where $\varphi_y(s) := f(x + sy)$. We then have the Taylor expansion, for instance up to order 2,

$$f(x + sy) = f(x) + s(\delta_x^{+, 1} f)(y) + \frac{1}{2}s^2(\delta_x^{+, 2} f)(y) + O(s^3).$$

B.2. **$k \cdot p$ perturbation method.** Perturbation theory in the Bloch momentum variable k is called the $k \cdot p$ method in physics literature [44, 53, 61, 72]. We recall it in this section.

Take $k \in \mathbb{R}^2 \setminus \{(0, 0)\}$, the goal of this section is to differentiate the eigenvectors of h_{K+sk} with respect to k , that is in the direction given by k . We define the operators

$$A(s) := h_{K+sk} = \frac{1}{2}(-i\nabla_{K+sk})^2 + v = A^0 + sA^1 + s^2A^2,$$

where

$$A^0 := \frac{1}{2}(-i\nabla_K)^2 + v, \quad A^1 := |k|D_k = k \cdot (-i\nabla_K), \quad A^2 := \frac{|k|^2}{2}. \quad (57)$$

Similarly as in Section A, let us assume that we start the perturbation from a level E^0 in which $\text{Ker}(A^0 - E^0)$ is of dimension 2, as in the graphene case, and that the degeneracy is lifted at first order, in any direction. We denote by $\mathbb{U}_\eta(q)$ the two eigenvectors of h_q , $\eta \in \{-, +\}$, defined for q locally around $q = K$, such that their eigenvalues at $q = K$ are E^0 , and such that the maps $U_{\eta, k}(s) := \mathbb{U}_\eta(K + sk)$ are smooth for s in a neighborhood of 0^+ . The corresponding eigenvalues of $\mathbb{U}_\eta(q)$ are denoted by $e_\eta(q)$, and $E_{\eta, k}(s) := e_\eta(K + sk)$.

For any $\ell \in \mathbb{N} \cup \{0\}$, we define the directional derivatives of \mathbb{U} and e at K in the direction k ,

$$U_{\eta,k}^\ell := (\delta_K^{+,\ell} \mathbb{U}_\eta)(k) = \left(\frac{d^\ell}{ds^\ell} U_{\eta,k} \right) \Big|_{s=0}, \quad E_{\eta,k}^\ell := (\delta_K^{+,\ell} e_\eta)(k) = \left(\frac{d^\ell}{ds^\ell} E_{\eta,k} \right) \Big|_{s=0}$$

for $\eta \in \{-, +\}$ and $\ell \in \{0, 1\}$. We have $U_\eta(s) = U_{\eta,k}^0 + sU_{\eta,k}^1$, $E_\eta(s) = E^0 + sE_{\eta,k}^1 + O(s^2)$. We define $k_{\mathbb{C}} := k_1 + ik_2 \in \mathbb{C}$. In the basis w_1, w_2 (defined in (6)), $(PA^1P)|_{P\mathcal{H} \rightarrow P\mathcal{H}}$ can be rewritten

$$\left(\langle w_i, A^1 w_j \rangle \right)_{1 \leq i, j \leq 2} = k \cdot \left(\langle w_i, (-i\nabla_K) w_j \rangle \right)_{1 \leq i, j \leq 2} \stackrel{(16)}{=} v_{\mathbb{F}} \sigma \cdot k$$

and its two eigenvalues are $E_{\eta,k}^1 = \eta v_{\mathbb{F}} |k|$.

We recall that for $\kappa \in \mathbb{C}$, the matrix $M := \begin{pmatrix} 0 & \kappa \\ \bar{\kappa} & 0 \end{pmatrix}$ has eigenvectors $g_\eta = \begin{pmatrix} \eta \frac{\kappa}{|\kappa|} & 1 \end{pmatrix}^T$, with $Mg_\eta = \eta |\kappa| g_\eta$, $\eta \in \{\pm\}$. Hence from Section A.3 we deduce that

$$U_{\eta,k}^0 = \frac{1}{\sqrt{2}} \left(\eta \frac{\bar{k}_{\mathbb{C}}}{|k|} w_1 + w_2 \right)$$

and $PA^1PU_{\eta,k}^0 = E_{\eta,k}^1 U_{\eta,k}^0$. The family $U_{\eta,k}^0$ is not continuous in k around $k = 0$. Moreover, from (56) we have

$$U_{\eta,k}^1 = |k| RD_k U_{\eta,k}^0 + \frac{\eta |k|}{2v_{\mathbb{F}}} \langle U_{-\eta,k}^0, D_k RD_k U_{\eta,k}^0 \rangle U_{-\eta,k}^0$$

and

$$E_n^1 = |k| \langle U_{\eta,k}^0, D_k U_{\eta,k}^0 \rangle, \quad E_n^2 = \frac{|k|^2}{2} + |k|^2 \langle U_{\eta,k}^0, D_k RD_k U_{\eta,k}^0 \rangle.$$

Finally

$$\begin{aligned} \mathbb{U}_\eta(K + k) &= \mathbb{U}_\eta \left(K + |k| \frac{k}{|k|} \right) = U_{\eta, \frac{k}{|k|}}^0 + |k| U_{\eta, \frac{k}{|k|}}^1 + O(|k|^2) \\ &= U_{\eta,k}^0 + U_{\eta,k}^1 + O(|k|^2). \end{aligned}$$

B.3. Building reduced spaces from perturbation theory. Avoiding the use of degenerate perturbation theory with eigenstates, we can use perturbation theory with density matrices, which is much simpler when the goal is only to generate the space spanned by perturbative eigenvectors. See [63] for the computation of coefficients in density matrix perturbation theory, and [40, Section 9] for a mathematical review.

Let us denote by $\Gamma_k(s)$ the orthogonal projection onto the space

$$\text{Span} \left(U_{\eta,k}(s) \right)_{\eta \in \{-, +\}}.$$

We expand it as $\Gamma_k(s) = \sum_{n=0}^{+\infty} s^n \Gamma_k^n$. We define

$$\mathcal{B}_{\ell,k} := \text{Span} \left(\left(U_{\eta,k}^m \right)_{\eta \in \{-, +\}}^{0 \leq m \leq \ell} \right)$$

which is the space spanned by the derivatives of the eigenvectors in the direction k . We are searching for two kinds of families, with the minimal number of vectors in each, $\mathcal{F}_{\ell,k}$ and \mathcal{F}_ℓ such that

$$\text{Span } \mathcal{F}_{\ell,k} = \mathcal{B}_{\ell, \frac{k}{|k|}}, \quad \text{Span } \mathcal{F}_\ell = \bigcup_{k \in \mathcal{B} \setminus \{0\}} \mathcal{B}_{\ell, \frac{k}{|k|}}. \quad (58)$$

Remark that $\text{Span } \mathcal{F}_{\ell,k} \subset \text{Span } \mathcal{F}_\ell$. Moreover, we have

$$\mathbb{U}_\eta(K + k) = U + O(|k|^{\ell+1}) \quad \text{where } U \in \text{Span } \mathcal{F}_{\ell,k} \subset \text{Span } \mathcal{F}_\ell.$$

The first kind of family will span the ‘‘perturbative space’’ in the direction $k/|k|$ up to order ℓ , and the second one will span it uniformly in k . From [40, Lemma 4.2] we have

$$\mathcal{B}_{\ell,k} = \text{Span} \left((\Gamma_k^n w_a)_{a \in \{1,2\}}^{0 \leq n \leq \ell} \right). \quad (59)$$

Now, since the derivatives Γ^n are easy to compute, we can obtain the space written on the left of the last equation. Let us do this up to second order. We use the notations (57). From [63] or [40, Section 9] we have

$$\begin{aligned} \Gamma_k^1 &= RA^1P + PA^1R, \\ \Gamma_k^2 &= RA^1PA^1R - PA^1R^2A^1P + RA^2P + PA^2R \\ &\quad + RA^1RA^1P + PA^1RA^1R - R^2A^1PA^1P - PA^1PA^1R^2, \end{aligned}$$

Remark that $\Gamma_k^0 = P$, which we denote by Γ^0 since it does not depend on k . Hence,

$$\begin{aligned} \Gamma_k^1 w_a &= |k| RD_k w_a, \\ \Gamma_k^2 w_a &= |k|^2 (-PD_k R^2 D_k w_a + (RD_k)^2 w_a - R^2 D_k P D_k w_a). \end{aligned}$$

We precise that $(RD_k)^2 = \sum_{a,b \in \{1,2\}} |k|^{-2} k_a k_b R(-i\partial_a)R(-i\partial_b)$.

For the second order,

$$\begin{aligned} \text{Im} (PD_k R^2 D_k w_a) &\subset \text{Span } \mathcal{F}_{1,k} \\ \text{Im} (R^2 D_k P D_k w_a) &\subset \text{Span} (R^2 D_k w_a)_{1 \leq a \leq 2}, \end{aligned}$$

Thus for the families defined in (17), we see that (58) and (59) are satisfied. Following this method, one can obtain reduced spaces families $\mathcal{F}_{\ell,k}$ and \mathcal{F}_ℓ at all perturbative orders ℓ . From [40, Lemma 4.2], except in exceptional cases where the corresponding family of vectors is not linearly independent (in which case we need less vectors), for any $\ell \in \mathbb{N} \cup \{0\}$ we need exactly $2(\ell+1)$ elements to build the family $\mathcal{F}_{\ell,k}$ at order ℓ . Hence $|\mathcal{F}_{\ell,k}| = M = 2(\ell+1)$.

APPENDIX C. SCHUR REDUCTION

In this section, we quickly recall the principle of the Schur reduction [78, 79], at a formal level. Consider two self-adjoint operators H and Y on a Hilbert space \mathcal{H} , take an orthogonal projection \mathbb{P} onto \mathcal{H} , define $\mathbb{P}^\perp := 1 - \mathbb{P}$, and assume that $\mathbb{P}Y\mathbb{P}^\perp = 0$. Let us denote by (E, ϕ) a non-degenerate solution

of the generalized eigenvalue problem associated to H and Y , so $H\phi = EY\phi$, and Y is called the mass operator. Then

$$(H - EY)\mathbb{P}\phi + (H - EY)\mathbb{P}^\perp\phi = 0. \quad (60)$$

Applying \mathbb{P}^\perp gives $\mathbb{P}^\perp(EY - H)\mathbb{P}^\perp\phi = \mathbb{P}^\perp H\mathbb{P}\phi$. Assume that there exists $\varepsilon > 0$ such that

$$\sigma\left(\left(\mathbb{P}^\perp(EY - H)\mathbb{P}^\perp\right)_{|\mathbb{P}^\perp\mathcal{H} \rightarrow \mathbb{P}^\perp\mathcal{H}}\right) \cap]-\varepsilon, \varepsilon[= \emptyset,$$

and define the partial inverse

$$r := \begin{cases} 0 & \text{on } \mathbb{P}\mathcal{H}, \\ \left(\left(\mathbb{P}^\perp(EY - H)\mathbb{P}^\perp\right)_{|\mathbb{P}^\perp\mathcal{H} \rightarrow \mathbb{P}^\perp\mathcal{H}}\right)^{-1}_\perp & \text{on } \mathbb{P}^\perp\mathcal{H}, \end{cases}$$

extended by linearity on all of \mathcal{H} . We have $r\mathbb{P}^\perp(EY - H)\mathbb{P}^\perp = \mathbb{P}^\perp$ so $\mathbb{P}^\perp\phi = rH\mathbb{P}\phi$. Applying \mathbb{P} to (60) and using $1 = \mathbb{P} + \mathbb{P}^\perp$ gives

$$\mathbb{P}(H + HrH - EY)\mathbb{P}\phi = 0, \quad \phi = (1 + rH)\mathbb{P}\phi. \quad (61)$$

This set of equations has to be seen in the following way : one of the generalized eigenmodes of the effective operator $\mathbb{P}(H + HrH)\mathbb{P}$ (with mass operator Y) is $(E, \mathbb{P}\phi)$, so once one has obtained it, one can obtain ϕ by applying $1 + rH$ to $\mathbb{P}\phi$. Thus, solving $\mathbb{P}(H + HrH)\mathbb{P}$ with mass operator Y leads to solve the exact operator H with mass operator Y .

C.1. Schur reduction applied to the effective operator. Then, with the same notations as in Section 4.10, we apply the Schur reduction with $H \leftarrow \mathbb{H}_k^\varepsilon$ (from 13), $Y \leftarrow \mathcal{S}$ and $\mathbb{P} \leftarrow P_2$. From (14), we have that

$$\begin{aligned} P_2\mathcal{M} = \mathcal{M}P_2 = 0, \quad P_2^\perp\mathcal{M}P_2^\perp = M, \quad P_2\mathcal{S}P_2^\perp = P_2^\perp\mathcal{S}P_2 = 0, \\ P_2\mathcal{L}P_2^\perp = T, \quad P_2^\perp\mathcal{L}P_2 = T^*. \end{aligned}$$

Hence we have formally

$$\begin{aligned} r &= P_2^\perp \left((E\mathcal{S} - \mathbb{H}_k^\varepsilon)_{|P_2^\perp\mathcal{H} \rightarrow P_2^\perp\mathcal{H}} \right)^{-1} P_2^\perp = -P_2^\perp (\varepsilon^{-1}(M + O(\varepsilon)))^{-1} P_2^\perp \\ &= -\varepsilon P_2^\perp M^{-1} P_2^\perp + O(\varepsilon^2). \end{aligned}$$

Hence

$$P_2\mathbb{H}_k^\varepsilon r \mathbb{H}_k^\varepsilon P_2 = -T \cdot (-i\nabla_k)(M^{-1}T^*) \cdot (-i\nabla_k) + O(\varepsilon).$$

and the effective operator (24). To reconstruct an approximation of the eigenvector of the original operator, one needs to form the quantity

$$\begin{aligned} (1 + r\mathbb{H}_k^\varepsilon)P_2 &= P_2 - \varepsilon \begin{pmatrix} 0 & 0 \\ 0 & M^{-1} \end{pmatrix} \mathbb{H}_k^\varepsilon P_2 + O(\varepsilon^2) \\ &= (1 - \varepsilon P_2^\perp M^{-1} T^*) P_2 + O(\varepsilon^2). \end{aligned}$$

REFERENCES

- [1] I. BABUŠKA AND R. LIPTON, *Optimal local approximation spaces for generalized finite element methods with application to multiscale problems*, Multiscale Model. Sim, 9 (2011), pp. 373–406.
- [2] I. BABUŠKA AND J. OSBORN, *Eigenvalue problems*, Elsevier, 1991.
- [3] G. BAL, P. CAZEAUX, D. MASSATT, AND S. QUINN, *Macroscopic approximation of tight-binding models near spectral degeneracies and validity for wave packet propagation*, arXiv preprint arXiv:2602.08073, (2026).
- [4] R. BALOG, B. JØRGENSEN, L. NILSSON, M. ANDERSEN, E. RIENKS, M. BIANCHI, M. FANETTI, E. LÆGSGAARD, A. BARALDI, S. LIZZIT, ET AL., *Bandgap opening in graphene induced by patterned hydrogen adsorption*, Nat. Mater, 9 (2010), pp. 315–319.
- [5] M. BARBIER, F. PEETERS, P. VASILOPOULOS, AND J. M. PEREIRA JR, *Dirac and Klein-Gordon particles in one-dimensional periodic potentials*, Phys. Rev. B, 77 (2008), p. 115446.
- [6] S. BECKER, M. EMBREE, J. WITTSTEN, AND M. ZWORSKI, *Mathematics of magic angles in a model of twisted bilayer graphene*, Probab. Math. Phys, 3 (2022), pp. 69–103.
- [7] S. BECKER, T. HUMBERT, AND M. ZWORSKI, *Integrability in the chiral model of magic angles*, Commun. Math. Phys, 403 (2023), pp. 1153–1169.
- [8] ———, *Fine structure of flat bands in a chiral model of magic angles*, in Ann. Henri Poincaré, Springer, 2024, pp. 1–31.
- [9] S. BECKER AND M. ZWORSKI, *Dirac points for twisted bilayer graphene with in-plane magnetic field*, J. Spectr. Theory, 14 (2024), pp. 479–511.
- [10] G. BERKOLAIKO AND A. COMECH, *Symmetry and Dirac points in graphene spectrum*, J. Spectr. Theory, 8 (2018), pp. 1099–1147.
- [11] O. L. BERMAN, G. GUMBS, AND Y. E. LOZOVIK, *Magnetoplasmons in layered graphene structures*, Phys. Rev. B, 78 (2008), p. 085401.
- [12] O. L. BERMAN, R. Y. KEZERASHVILI, AND Y. E. LOZOVIK, *Collective properties of magnetobieexcitons in quantum wells and graphene superlattices*, Phys. Rev. B, 78 (2008), p. 035135.
- [13] J. BEZANSON, A. EDELMAN, S. KARPINSKI, AND V. B. SHAH, *Julia: A fresh approach to numerical computing*, SIAM review, 59 (2017), pp. 65–98.
- [14] Í. S. BEZERRA AND J. R. LIMA, *Effects of fermi velocity engineering in magnetic graphene superlattices*, Phys. E: Low-Dimens. Syst. Nanostructures, 123 (2020), p. 114171.
- [15] R. BISTRITZER AND A. H. MACDONALD, *Moiré bands in twisted double-layer graphene*, Proc. Natl. Acad. Sci, 108 (2011), pp. 12233–12237.
- [16] Y. P. BLOKH, V. FREILIKHER, S. SAVEL’EV, AND F. NORI, *Transport and localization in periodic and disordered graphene superlattices*, Phys. Rev. B, 79 (2009), p. 075123.
- [17] S. BOYAVAL, *Reduced-basis approach for homogenization beyond the periodic setting*, Multiscale Model. Sim, 7 (2008), pp. 466–494.
- [18] L. BREY AND H. FERTIG, *Emerging zero modes for graphene in a periodic potential*, Phys. Rev. Lett, 103 (2009), p. 046809.
- [19] P. BURSET, A. L. YEYATI, L. BREY, AND H. FERTIG, *Transport in superlattices on single-layer graphene*, Phys. Rev. B, 83 (2011), p. 195434.
- [20] V. S. BUSLAEV, *Semiclassical approximation for equations with periodic coefficients*, Russ. Math. Surv, 42 (1987), p. 97.
- [21] É. CANCÈS, L. GARRIGUE, AND D. GONTIER, *Simple derivation of moiré-scale continuous models for twisted bilayer graphene*, Phys. Rev. B, 107 (2023), p. 155403.
- [22] E. CANCÈS AND L. MENG, *Semiclassical analysis of two-scale electronic hamiltonians for twisted bilayer graphene*, arXiv preprint arXiv:2311.14011, (2023).
- [23] S. CARR, D. MASSATT, S. FANG, P. CAZEAUX, M. LUSKIN, AND E. KAXIRAS, *Twistronics: Manipulating the electronic properties of two-dimensional layered structures through their twist angle*, Phys. Rev. B, 95 (2017), p. 075420.

- [24] J. CHEN, D. MA, AND Z. ZHANG, *A multiscale reduced basis method for the Schrödinger equation with multiscale and random potentials*, Multiscale Model. Simul, 18 (2020), pp. 1409–1434.
- [25] S.-C. CHEN, R. KRAFT, R. DANNEAU, K. RICHTER, AND M.-H. LIU, *Electrostatic superlattices on scaled graphene lattices*, Commun. Phys, 3 (2020), p. 71.
- [26] E. CHUNG, Y. EFENDIEV, AND T. Y. HOU, *Multiscale Model Reduction*, Springer, 2023.
- [27] C. DEAN, A. YOUNG, L. WANG, I. MERIC, G.-H. LEE, K. WATANABE, T. TANIGUCHI, K. SHEPARD, P. KIM, AND J. HONE, *Graphene based heterostructures*, Solid State Commun, 152 (2012), pp. 1275–1282.
- [28] L. DELL’ANNA AND A. DE MARTINO, *Multiple magnetic barriers in graphene*, Phys. Rev. B, 79 (2009), p. 045420.
- [29] ———, *Magnetic superlattice and finite-energy Dirac points in graphene*, Phys. Rev. B, 83 (2011), p. 155449.
- [30] M. DIMASSI, *Développements asymptotiques des perturbations lentes de l’opérateur de Schrödinger périodique*, Commun. Partial Differ. Equ, 18 (1993), pp. 771–803.
- [31] T. DUGUET, A. EKSTRÖM, R. J. FURNSTAHL, S. KÖNIG, AND D. LEE, *Colloquium: Eigenvector continuation and projection-based emulators*, Rev. Mod. Phys, 96 (2024), p. 031002.
- [32] Y. EFENDIEV AND T. Y. HOU, *Multiscale finite element methods: theory and applications*, vol. 4, Springer Science & Business Media, 2009.
- [33] M. FARJAM, *Visualizing the influence of point defects on the electronic band structure of graphene*, J. Condens. Matter Phys, 26 (2014), p. 155502.
- [34] C. FEFFERMAN, J. LEE-THORP, AND M. WEINSTEIN, *Honeycomb Schrödinger operators in the strong binding regime*, Comm. Pure Appl. Math, 71 (2018), pp. 1178–1270.
- [35] C. FEFFERMAN AND M. WEINSTEIN, *Honeycomb lattice potentials and Dirac points*, J. Am. Math. Soc, 25 (2012), pp. 1169–1220.
- [36] C. L. FEFFERMAN AND M. I. WEINSTEIN, *Wave packets in honeycomb structures and two-dimensional Dirac equations*, Commun. Math. Phys, 326 (2014), pp. 251–286.
- [37] D. E. FERNANDES, *Effective medium model for graphene superlattices with electrostatic and magnetic vector potentials*, Phys. Rev. B, 107 (2023), p. 085119.
- [38] D. E. FERNANDES, M. RODRIGUES, G. FALCÃO, AND M. G. SILVEIRINHA, *Time evolution of electron waves in graphene superlattices*, AIP Advances, 6 (2016).
- [39] D. FRAME, R. HE, I. IPSEN, D. LEE, D. LEE, AND E. RRAPAJ, *Eigenvector continuation with subspace learning*, Phys. Rev. Lett., 121 (2018), p. 032501.
- [40] L. GARRIGUE AND B. STAMM, *On reduced basis methods for eigenvalue problems, and on its coupling with perturbation theory*, arXiv preprint arXiv:2408.11924, (2024).
- [41] C. GÉRARD, A. MARTINEZ, AND J. SJÖSTRAND, *A mathematical approach to the effective Hamiltonian in perturbed periodic problems*, Commun. Math. Phys, 142 (1991), pp. 217–244.
- [42] P. GÉRARD, P. A. MARKOWICH, N. J. MAUSER, AND F. POUPAUD, *Homogenization limits and Wigner transforms*, Commun. Pure Appl. Math, 50 (1997), pp. 323–379.
- [43] J. GUILLOT, J. RALSTON, AND E. TRUBOWITZ, *Semi-classical asymptotics in solid state physics*, Commun. Math. Phys, 116 (1988), pp. 401–415.
- [44] W. A. HARRISON, *Electronic structure and the properties of solids: the physics of the chemical bond*, Courier Corporation, 2012.
- [45] M. F. HERBST, A. LEVITT, AND E. CANCÈS, *DFTK: A Julia approach for simulating electrons in solids*, Proc. JuliaCon Conf., 3 (2021), p. 69.
- [46] J. HERNÁNDEZ, J. OLIVER, A. E. HUESPE, M. CAICEDO, AND J. CANTE, *High-performance model reduction techniques in computational multiscale homogenization*, Comput. Methods Appl. Mech. Eng, 276 (2014), pp. 149–189.
- [47] J. O. HIRSCHFELDER, *Formal Rayleigh–Schrödinger perturbation theory for both degenerate and non-degenerate energy states*, Int. J. Quantum Chem, 3 (1969), pp. 731–748.
- [48] T. HOU, X.-H. WU, AND Z. CAI, *Convergence of a multiscale finite element method for elliptic problems with rapidly oscillating coefficients*, Math. Comput, 68 (1999), pp. 913–943.

- [49] A. ISACSSON, L. M. JONSSON, J. M. KINARET, AND M. JONSON, *Electronic superlattices in corrugated graphene*, Phys. Rev. B, 77 (2008), p. 035423.
- [50] T. KATO, *Perturbation theory for linear operators*, Springer, second ed., 1995.
- [51] M. I. KATSNELSON, *The Physics of Graphene*, Cambridge University Press, 2 ed., 2020.
- [52] M. KINDERMANN, B. UCHOA, AND D. L. MILLER, *Zero-energy modes and gate-tunable gap in graphene on hexagonal boron nitride*, Phys. Rev. B, 86 (2012), p. 115415.
- [53] C. KITTEL, *Quantum Theory of Solids*, John Wiley & Sons, 2nd ed., 1987.
- [54] T. KONG, D. LIU, M. LUSKIN, AND A. B. WATSON, *Modeling of electronic dynamics in twisted bilayer graphene*, SIAM J. Appl. Math, 84 (2024), pp. 1011–1038.
- [55] W. KU, T. BERLIJN, AND C.-C. LEE, *Unfolding first-principles band structures*, Phys. Rev. Lett, 104 (2010), p. 216401.
- [56] L. D. LANDAU, E. M. LIFŠIĆ, E. M. LIFSHITZ, A. M. KOSEVICH, AND L. P. PITAEVSKII, *Theory of elasticity: volume 7*, vol. 7, Elsevier, 1986.
- [57] V. Q. LE, C. H. PHAM, AND V. L. NGUYEN, *Magnetic Kronig–Penney-type graphene superlattices: finite energy Dirac points with anisotropic velocity renormalization*, J. Condens. Matter Phys, 24 (2012), p. 345502.
- [58] M. P. LEVENDORF, C.-J. KIM, L. BROWN, P. Y. HUANG, R. W. HAVENER, D. A. MULLER, AND J. PARK, *Graphene and boron nitride lateral heterostructures for atomically thin circuitry*, Nature, 488 (2012), pp. 627–632.
- [59] Y. LI, S. DIETRICH, C. FORSYTHE, T. TANIGUCHI, K. WATANABE, P. MOON, AND C. R. DEAN, *Anisotropic band flattening in graphene with one-dimensional superlattices*, Nat. Nanotechnol, 16 (2021), pp. 525–530.
- [60] LI, PANCHI AND ZHANG, ZHIWEN, *Efficient finite element methods for semiclassical nonlinear Schrödinger equations with random potentials*, ESAIM: M2AN, 59 (2025), pp. 3249–3281.
- [61] J. M. LUTTINGER AND W. KOHN, *Motion of electrons and holes in perturbed periodic fields*, Phys. Rev, 97 (1955), p. 869.
- [62] S. G. MAYO, F. YNDURAIN, AND J. M. SOLER, *Band unfolding made simple*, J. Condens. Matter Phys, 32 (2020), p. 205902.
- [63] R. MCWEENEY, *Perturbation theory for the Fock-Dirac density matrix*, Phys. Rev, 126 (1962), p. 1028.
- [64] G. G. NAUMIS, *Electronic properties of two-dimensional materials*, in Synthesis, Modeling, and Characterization of 2D Materials, and Their Heterostructures, Elsevier, 2020, pp. 77–109.
- [65] N. NGUYEN, *A multiscale reduced-basis method for parametrized elliptic partial differential equations with multiple scales*, J. Comput. Phys, 227 (2008), pp. 9807–9822.
- [66] A. K. NOOR AND H. E. LOWDER, *Approximate techniques of structural reanalysis*, Comput. Struct, 4 (1974), pp. 801–812.
- [67] M. OHLBERGER AND F. SCHINDLER, *Error control for the localized reduced basis multiscale method with adaptive on-line enrichment*, SIAM J. Sci. Comput, 37 (2015), pp. A2865–A2895.
- [68] C. ORTIX, L. YANG, AND J. VAN DEN BRINK, *Graphene on incommensurate substrates: Trigonal warping and emerging Dirac cone replicas with halved group velocity*, Phys. Rev. B, 86 (2012), p. 081405.
- [69] G. PANATI, H. SPOHN, AND S. TEUFEL, *Effective dynamics for Bloch electrons: Peierls substitution and beyond*, Commun. Math. Phys, 242 (2003), pp. 547–578.
- [70] C.-H. PARK, L. YANG, Y.-W. SON, M. L. COHEN, AND S. G. LOUIE, *Anisotropic behaviours of massless Dirac fermions in graphene under periodic potentials*, Nat. Phys, 4 (2008), pp. 213–217.
- [71] ———, *New generation of massless Dirac fermions in graphene under external periodic potentials*, Phys. Rev. Lett, 101 (2008), p. 126804.
- [72] Y. PETER AND M. CARDONA, *Fundamentals of semiconductors: physics and materials properties*, Springer Science & Business Media, 2010.
- [73] J. QUAN, N. RYBIN, M. SCHEFFLER, AND C. CARBOGNO, *Efficient band structure unfolding with atomic-centered orbitals: General theory and application*, arXiv preprint arXiv:2506.21089, (2025).

- [74] X. QUAN, A. B. WATSON, AND D. MASSATT, *Construction and accuracy of electronic continuum models of incommensurate bilayer 2d materials*, Electron. Struct, 7 (2025), p. 035005.
- [75] S. QUINN, T. KONG, M. LUSKIN, AND A. B. WATSON, *Higher-order continuum models for twisted bilayer graphene*, arXiv preprint arXiv:2502.08120, (2025).
- [76] M. RAMEZANI MASIR, P. VASILOPOULOS, A. MATULIS, AND F. PEETERS, *Direction-dependent tunneling through nanostructured magnetic barriers in graphene*, Phys. Rev. B, 77 (2008), p. 235443.
- [77] M. REED AND B. SIMON, *Methods of Modern Mathematical Physics. IV. Analysis of operators*, Academic Press, New York, 1978.
- [78] I. SCHUR, *Über die Verteilung der Wurzeln bei gewissen algebraischen Gleichungen mit ganzzahligen Koeffizienten*, Math. Z., 1 (1918), pp. 377–402.
- [79] J. SCHUR, *Über potenzreihen, die im innern des einheitskreises beschränkt sind.*, J. Reine Angew. Math, 1918 (1918), pp. 122–145.
- [80] M. G. SILVEIRINHA AND N. ENGHETA, *Effective medium approach to electron waves: Graphene superlattices*, Phys. Rev. B, 85 (2012), p. 195413.
- [81] L.-G. WANG AND S.-Y. ZHU, *Electronic band gaps and transport properties in graphene superlattices with one-dimensional periodic potentials of square barriers*, Phys. Rev. B, 81 (2010), p. 205444.
- [82] A. B. WATSON, T. KONG, A. H. MACDONALD, AND M. LUSKIN, *Bistritzer–MacDonald dynamics in twisted bilayer graphene*, J. Math. Phys, 64 (2023).
- [83] R. WINKLER AND U. ZÜLICHE, *Invariant expansion for the trigonal band structure of graphene*, Phys. Rev. B, 82 (2010), p. 245313.
- [84] Q.-P. WU, Z.-F. LIU, A.-X. CHEN, X.-B. XIAO, AND G.-X. MIAO, *Tunable Dirac points and high spin polarization in ferromagnetic-strain graphene superlattices*, Sci. Rep, 7 (2017), p. 14636.
- [85] S. WU, M. KILLI, AND A. PARAMAKANTI, *Graphene under spatially varying external potentials: Landau levels, magnetotransport, and topological modes*, Phys. Rev. B, 85 (2012), p. 195404.
- [86] J.-H. YUAN, J.-J. ZHANG, Q.-J. ZENG, J.-P. ZHANG, AND Z. CHENG, *Tunneling of Dirac fermions in graphene through a velocity barrier with modulated by magnetic fields*, Physica B Condens. Matter, 406 (2011), pp. 4214–4220.

LABORATOIRE “ANALYSE GÉOMÉTRIE MODÉLISATION”, CY CERGY PARIS UNIVERSITÉ,
95302 CERGY-PONTOISE, FRANCE

Email address: louis.garrigue@cyu.fr